NACA RM E52E05

NACA

RESEARCH MEMORANDUM

DESIGN AND TEST OF MIXED-FLOW IMPELLERS

I - AERODYNAMIC DESIGN PROCEDURE

By Walter M. Osborn and Joseph T. Hamrick

Lewis Flight Propulsion Laboratory
Cleveland, Ohio

NATIONAL ADVISORY COMMITTEE
FOR AERONAUTICS

WASHINGTON

September 19, 1952

1C NACA RM E52E05

NATIONAL ADVISORY COMMITTEE FOR AERONAUTICS

RESEARCH MEMORANDUM

DESIGN AND TEST OF MIXED-FLOW IMPELLERS

I - AERODYNAMIC DESIGN PROCEDURE

By Walter M. Osborn and Joseph T. Hamrick

SUMMARY

A mixed-flow impeller was designed using recently available techniques with special emphasis on the reduction or elimination of velocity deceleration along the wetted surfaces, especially along the blade suction surface. With a given hub-shroud profile, the blade shape at the blade mean height was determined from a prescribed velocity distribution on the blade surface for isentropic flow with the aid of the preliminary assumption of uniform flow conditions from hub to shroud. The blade shape at all other locations was fixed by the introduction of radial blade elements and blade taper which were specified in consideration of stress requirements.

In order to determine the velocities throughout the passage from the hub to the shroud, the over-all flow configuration was investigated by the use of an analysis in the hub-shroud plane in which axially symmetrical isentropic flow was assumed. The analysis method was extended to obtain the blade surface velocity distribution throughout the passage and to make comparisons at the blade mean height.

Impellers designed for an average velocity acceleration from inlet to outlet have relatively low outlet blade heights which may result in losses due to secondary flow and clearance effects. In order to allow for viscous effects (such as effective decrease in flow area) and to increase the blade-height-to-passage-width ratio, the blade height was arbitrarily increased. Splitter vanes were added to increase further the blade-height-to-passage-width ratio. Preliminary experimental results show that an impeller designed by this procedure had higher than average efficiency and good operating characteristics.

INTRODUCTION

Research on centrifugal compressors at the NACA Lewis laboratory is being conducted to evolve reliable design procedures which will eliminate the large amount of experimental development now necessary on new designs and will increase the centrifugal-compressor efficiency. In the development of design procedures it is necessary to investigate certain parameters that affect the flow when viscosity is considered. Because of

viscosity, parameters such as blade loading and blade-height-to-passage-width ratio become very important. In order to investigate these parameters and their various effects upon over-all performance, a series of mixed-flow impellers is being designed and tested. An attempt is being made to conduct the investigation in such a manner that the results will lead to improved design techniques. The procedure followed in the application of recent design and analysis methods to the design of the first of these impellers, designated the MFI-1, is presented herein.

In the design, an attempt was made to reduce or to eliminate, wherever possible, any velocity decelerations along the wetted surfaces, especially along the blade trailing face. Theoretical analysis (reference 1) and experimental investigations (references 2 and 3) indicate that although substantial decelerations along the impeller blade driving face (pressure surface) may be tolerated, decelerations along the blade trailing face (suction surface) may result in severe losses.

The MFI-1 impeller was designed to give a blade shape with a prescribed blade surface-velocity distribution at the mean blade height by the method of reference 4. The blade shape at all other locations was fixed by the introduction of radial blade elements and blade taper which were specified in consideration of stress requirements. The effect of the hub-shroud curvature on the velocity distribution and the compromises in geometric design necessitated by stress restrictions were investigated by an analysis in the meridional (hub-shroud) plane by the method of reference 5.

In order to allow for viscous effects, such as effective decrease in area, and to increase the blade-height-to-passage-width ratio, the blade height was arbitrarily increased and splitter vanes were added for the first test version of the experimental impeller designated the MFI-1A. These design changes will be eliminated by successive steps in the experimental impeller in order to obtain a better estimate of the allowances that should be made.

The geometric coordinates for the design (MFI-1) and the modified (MFI-1A) impellers are given in table I and the experimental performance characteristics of the MFI-1A are presented in figure 1.

DESIGN PROCEDURE

In the design procedure, the design method of reference 4 and the analysis method of reference 5, both of which are for isentropic compressible flow, were used to arrive at the design of the MFI-1. In order to use this design procedure, complete familiarity with both references is necessary.

[redacted]

Basically, reference 4 is a blade design method and was used to design the blade at mean passage height. The height ratio H^* required by the design method of reference 4 was used to determine a provisional hub-shroud profile. (All symbols used herein are given in appendix A.) With radial blade elements the blade shape may be specified at only one radial location, for example, mean blade height. The radial elements and specified blade taper determine the blade shape at all other points.

The provisional hub-shroud profile was determined by the assumption, in effect, that flow conditions are uniform normal to the mean surface of revolution. In order to determine the effect of this assumption, the method of reference 5 was used to investigate the variation in flow conditions from hub to shroud and to determine the resulting changes in hub-shroud profile required to obtain the desired flow rate and velocity distribution. An extension of this method was used to determine the blade surface velocities over the entire blade.

Blade-Shape Design

The initial blade shape for the MFI-1 was determined by the first approximation of the design method of reference 4 (the assumption that the mass-weighted average flow direction is equal to the direction of the blade camber line at mean blade height).

Inlet and outlet conditions. - The following conditions were specified:

Impeller outlet mean-line speed (7.00 in. outlet mean radius), ft/sec	1400
Design flow rate (for 14 in. outlet mean diameter), lb/sec	15.3
Slip factor (from backward curved blades at outlet)	0.90
Prerotation, λ	0
Inlet radius at shroud, in.	4.725
Inlet radius at hub, in.	1.678

From continuity relations and the given conditions, the following quantities were determined:

Axial inlet velocity, ft/sec	547
Relative velocity q at mean inlet radius, ft/sec	843

The relative velocity q at the mean radius at the outlet was arbitrarily set 10 percent higher than the inlet relative velocity to give an average acceleration from inlet to outlet. An approximate cone angle of 30° at discharge was specified for a first approximation.

Provisional hub-shroud shape. - A provisional mean line similar to that shown in figure 2 was drawn from the inlet mean radius to the outlet mean radius maintaining approximately a 30° angle with the axis of rotation. Blade height lines h perpendicular to the mean line were added at equal intervals symmetrical about the mean line. The value of h at the inlet was taken equal to the annulus height and the h value at the outlet was fixed by continuity relations from the specified operating conditions. Lines faired in through the extremities of these h lines formed the provisional hub and shroud shapes. The ratio of these h values to h at the outlet was used for the value of H^* in the method of reference 4. Thus, in effect, it was assumed that if continuity were satisfied for a flow filament having the prescribed variation in H^* along the mean surface of revolution, continuity would also be satisfied for an entire annulus having a hub-to-shroud spacing determined by the prescribed h values. This assumption is true if the flow conditions are uniform along each h line and the blade thickness in percentage of blade spacing is constant (inverse blade taper).

Velocity distribution. - With the use of the inlet and outlet relative velocities as specified as end points, a prescribed mean-line velocity distribution along the blade driving and trailing faces was drawn with minimum rate of deceleration near the outlet along the trailing face as shown in figure 3. The ratio of the relative velocity at any point to the velocity of sound at inlet stagnation conditions Q is plotted against L, the ratio of the distance along the mean line to the total mean-line length. These velocity ratios are prescribed along the mean-line surface of revolution only.

The velocity diagram was checked to determine whether the resulting blade loading provided a uniform spacing of blades and finite thicknesses. It was necessary to modify the velocity diagram in order to eliminate fractional blades and to provide thickness at inlet and outlet as required for structural reasons and for providing a rounded leading edge at inlet. The final velocity diagram is the one shown in figure 3.

Blade shape. - From the prescribed conditions, the blade shape lying on the mean-line surface of revolution was obtained by the method of reference 4. The final blade shape was drawn on a developed surface of revolution which closely approximated that of the mean line and is shown in figure 4. For this impeller, thin blades were desired because thick blades which are tapered in the conventional manner, as in the MFI-1, produce a larger reduction in percentage of available flow area at the hub. In order to produce the desired blade thickness, it was necessary to vary the blade height h in successive solutions. Variation of the blade height to produce the relatively thin blade shown in figure 4 resulted in the provisional hub-shroud shape drawn through the extremities of the h lines in figure 2.

[redacted]

Composite blade shape. - A mean camber surface was formed by passing radial lines through the blade camber line on the mean-line surface of revolution (fig. 4). The radial blade element was formed as shown by the broken lines in figure 5. The thickness of the blade at the mean blade-height line resulted from the design method, and a 3° taper determined the thickness at all other points except where the taper had to be reduced slightly in order to provide adequate thickness at the shroud and to relieve the thickness at the hub near the inlet.

Final Hub-Shroud Shape

It was realized that the uniform conditions from hub to shroud which were assumed in the use of reference 4 would not be obtained and that compensating adjustments in the provisional hub-shroud profile would be necessary. In order to determine the departure from uniform conditions and to determine the effect of this departure on the velocity distribution along the mean line, an analysis was made in the hub-shroud plane by the method of reference 5.

A preliminary analysis indicated that the initially specified weight flow of 15.3 pounds per second could not be reached even with extensive modification. A slight change in the hub shape was made to allow a maximum flow of 14.5 pounds per second. The final hub-shroud shape is shown in figure 2. Analyses of the flow were made at weight flows of 13.0 and 14.5 pounds per second, at 1400 feet per second outlet mean-line speed. A comparison of the two weight flows indicated very little difference in general trend. The results of the analysis for the flow rate of 14.5 pounds per second are shown in figures 6 and 7.

Streamlines and normals. - The flow streamlines and normals in the meridional plane are shown in figure 6(a). The solution was made along the normals shown for 20 stream tubes in the first one-third of the impeller passage and for 10 stream tubes thereafter with equal weight flows through the stream tubes.

Meridional velocity distribution. - Lines of constant velocity ratio Q relative to the impeller in the meridional plane are shown in figure 6(b). The flow accelerates along the hub throughout the impeller. Apparently, the maintenance of accelerating flow conditions along the hub is not difficult, if the flow is accelerated on the average; however, not many impellers have been designed to eliminate this possible source of boundary-layer losses, and a good example of this is the impeller analyzed in reference 5. The poor performance of that impeller was attributed in part to these decelerations. Because of the high relative velocities at inlet near the shroud, decelerations along the shroud could not be avoided in the first half of the impeller although excessive decelerations in this region probably contribute losses just as great or greater than the losses at the hub.

Blade surface velocity distribution. - The method of reference 5 has been extended in appendix B of this report in order to obtain the blade surface-velocity distribution for a finite number of blades. By the use of the tangential component of the blade-force term to compute the pressure difference and the assumption that a linear variation of pressure exists across the blade passage, the blade surface pressure distribution was obtained. From the pressure distribution, the blade surface velocity distribution was computed. The theoretical blade surface velocity diagrams for flow streamlines (fig. 6(a)) 0 (hub), 4, 8, 12, 16, and 20 (shroud) are presented in figure 7. Because a linear variation in pressure across the passage was assumed in the derivation of the equations, a nonlinear variation of velocity results. The mean velocity shown in figure 7 therefore will not be the arithmetical mean of the driving- and trailing-face velocities. Streamline 8 lies closest to the mean blade-height line shown in figure 2. A comparison of the prescribed velocity diagram of figure 3 with the velocity diagram at streamline 8 (fig. 7(c)) shows a good agreement in the diagram configuration for the distance ratios L above 0.3 provided that the average velocity in figure 7(c) is increased to account for the higher weight flow in figure 3.

The rapid rise in velocity near the inlet (for example, fig. 7(f)) was caused by only a moderate decrease in flow area. The flow near the shroud at the inlet is in the vicinity of sonic velocity with the result that small changes in passage flow area require large changes in velocity in order to maintain constant weight flow. The blade surface decelerations between the distance ratios of 0.1 and 0.3 (figs. 7(b) to 7(f)) probably could be tolerated as the boundary layer in the inlet section should be small.

Meridional pressure distribution. - Lines of constant pressure ratio (ratio of local static pressure to inlet total pressure) are shown in figure 6(c). The existence of pressure ratios greater than 1 at the hub and decreasing to below 1 at the shroud indicate an axial velocity increase from hub to shroud at the impeller inlet. This results from the assumption that the mass-weighted average flow direction is equal to the direction of the blade camber line and may be explained as follows:

The fact that the static pressure in the inlet is higher than the total pressure upstream of the blades indicates a sudden addition of energy to the flow. When perfect guidance is assumed, sudden additions in energy are always obtained for positive angles of attack (fluid approaches driving face of the blade). The pressure ratios greater than 1 at the hub decreasing to less than 1 at the shroud thus indicate that the velocity gradient is such as to give a decreasing angle of attack from hub to shroud. If the velocity is uniform from hub to shroud, the pressure ratio increases from hub to shroud for velocities below that required for zero angle of attack.

Angle of attack. - The angle of attack is defined as the angle between the flow direction of the air at inlet and the blade camber line, with flow directed at the driving face of the blade forming a positive angle of attack. The pressure variation at the inlet (fig. 6(c)) indicates the existence of a positive angle of attack. Extension of the analysis upstream of the impeller was difficult because of the discontinuities due to flow angle and blade thickness. Analyses were therefore made of the flow between the hub and the shroud with no rotation and no blades for weight flows of 13.0 and 14.5 pounds per second to determine the effect of the hub and shroud curvatures upon the entering flow. The hub-shroud profile was assumed to produce a much greater effect upon the inlet flow configuration than blade thickness and taper. If this assumption was true, the angle of attack as determined from the flow through the hub-shroud annulus should have been very similar to the angle of attack approaching the rotating impeller. The angle of attack as computed in this manner for the two weight flows is shown in figure 8.

For uniform axial velocity in the inlet annulus, blades having radial elements are necessary in order to produce the condition of zero angle of attack at all radial positions along the blade. If, as in the case of the MFI-1 impeller, the axial velocity is lower at the hub than at the shroud, it is probably desirable to sweep the leading edge back from hub to shroud in order to maintain zero angle of attack.

Maximum weight flow. - Maximum weight flow was computed for a range of exit mean-line speeds and is presented in figure 9. The solution at 1400 feet per second showed that choking occurred prior to a distance ratio of 0.3 along the mean line. Choking in this region is attributed to the large inlet blade angles. For large blade angles at the shroud, very high velocities relative to the blade may be required to provide the meridional velocity component necessary to pass the design weight flow. For compressible fluids where the relative velocity becomes supersonic, the level of velocity across the passage is increased because of the increased area required for the supersonic velocity and premature choking results. For large blade heights and large blade angles, radial blade elements produced a large increase in blade angle from hub to shroud. Therefore, if the inlet blade angle at the mean line is large, the effect of the much larger blade angle at the shroud becomes significant in regard to maximum weight flow.

Because of the angle-of-attack effects previously discussed and because of the present maximum weight-flow considerations, the inlet section of a mixed-flow impeller can be concluded to impose the greatest problem in design.

The point of maximum flow restriction moved from the inlet to the outlet as the speed was decreased from 1400 to 700 feet per second because of the general decrease in density level with decreasing speed.

At tip speeds lower than 1100 feet per second, the restriction at the outlet was greater than at the inlet. Because of the time required, the exact location of choking was not determined at speeds other than 1400 feet per second.

MODIFIED IMPELLER MFI-1A

Impellers designed for an average velocity acceleration from inlet to outlet (for example, MFI-1) have relatively low blade-height-to-passage-width ratios toward the outlet which may result in increased losses because of secondary flow and clearance effects. The evaluation of the effects in an impeller due to viscosity, secondary flows, and leakage through the blade-to-shroud clearance space is difficult; however, as the design and analysis methods are both for isentropic flow, agreement between the theoretical analysis and experimental results can not be expected unless some modifications are made to allow for these effects. From analyses of other compressors, the theoretical static pressure was found to be increasingly greater than the experimental static pressure from inlet to outlet. The difference in static pressures was assumed to be due to viscous effects which caused an effective decrease in flow area. The effective decrease in area is taken as that due to both boundary layer and decreased density caused by viscous losses. In accordance with this assumption, the blade height of the MFI-1 was increased 74 percent at the exit to allow for these effects (fig. 2) and to increase the blade-height-to-passage-width ratio. Splitter vanes were added near the outlet in order to obtain a further increase in blade-height-to-passage-width ratio. These design changes will be eliminated by successive steps in the experimental impeller in order to obtain a better estimate of the allowances that should be made. The resulting modified impeller was designated the MFI-1A, a front view and an over-all view of which are shown in figures 10 and 11, respectively.

An analysis was made of the MFI-1A (excluding the splitter vanes) in order to compare the velocity configurations for the MFI-1 and the MFI-1A. The streamline configuration for the MFI-1A is shown in figure 12. A comparison of the static pressures along the shroud is shown in figure 13 for a weight flow of 13.0 pounds per second and a comparison of the velocity distributions are shown in figure 14. Because of the similarity of the solutions for the weight flows of 13.0 and 14.5 pounds per second in the MFI-1, the solution at 14.5 pounds per second was not made for the MFI-1A.

The geometrical coordinates for the MFI-1 and MFI-1A are given in table I and the over-all performance of the MFI-1A is shown in figure 1. Preliminary experimental results (reference 6) show that the MFI-1A impeller had higher than average efficiency and good operating characteristics.

TIME REQUIRED

After the computation was set up, approximately 6 to 8 hours were required by an experienced computer to arrive at a blade shape from a given blade-height variation and prescribed velocity diagram by the method of reference 4. In the analysis of the initial design, approximately 120 hours were required by an engineer working with an experienced computer in setting up the computation by the method of reference 5 and arriving at enough information to establish the premature choking condition at the inlet. Approximately 500 hours of computing time and periodic supervision by the engineer were required to make a complete analysis.

CONCLUDING REMARKS

A mixed-flow impeller was designed with special emphasis upon the reduction or elimination of velocity decelerations along the wetted surface, especially along the blade suction surface. With the use of a provisional hub-shroud profile, the blade shape at the blade mean height was determined from a prescribed velocity distribution. The blade shape at all other locations was fixed by the introduction of radial blade elements and blade taper which were specified in consideration of stress requirements.

The variation in flow conditions from hub to shroud and the changes in the hub-shroud profile required in order to obtain the desired flow rate were investigated by an analysis in the hub-shroud plane in which axially symmetrical flow was assumed. The method was extended to obtain the blade surface-velocity distribution for a finite number of blades. From the analysis, the following conclusions were drawn:

Mixed-flow impellers may be designed for accelerating flow along the hub from inlet to outlet, but decelerations along the shroud cannot be avoided if the relative velocity is high at the inlet tip.

Impellers designed for an average velocity acceleration from inlet to outlet have relatively low blade-height-to-passage-width ratios toward the outlet which may result in increased losses because of secondary flow and clearance effects; however, increase in blade height to allow for effective decrease in area may reduce such losses.

For mixed-flow impeller blades designed by the method of reference 4 and with provisional hub-shroud profiles as used in the design procedure of this report, the variation in flow conditions from hub to shroud require that the hub-shroud profile be altered in order to obtain the desired flow rate.

The inlet section of a mixed-flow impeller imposes the greatest problem in design.

In order to allow for viscous effects and to increase the blade-height-to-passage-width ratio, the blade height was arbitrarily increased and splitter vanes were added. Preliminary experimental results show that an impeller designed by this procedure had higher than average efficiency and good operating characteristics.

Lewis Flight Propulsion Laboratory
National Advisory Committee for Aeronautics
Cleveland, Ohio

[redacted]

APPENDIX A

SYMBOLS

The following symbols are used in this report:

c	speed of sound for stagnation conditions, ft/sec
F	force per unit mass
f	factor accounting for area taken up by blade cross section
g	acceleration due to gravity, ft/sec^2
H	absolute total enthalpy, Btu/lb
H^*	ratio of blade height at any point to blade height at outlet
h	blade height perpendicular to mean blade-height line (fig. 2)
J	mechanical equivalent of heat
L	ratio of distance m at any point to m at impeller outlet
m	distance along streamline from inlet, ft
N	number of blades
P	total pressure, lb/sq ft
p	static pressure, lb/sq ft
Q	velocity ratio, q/c_i
q	velocity relative to impeller, ft/sec
r	radius of particle from axis of impeller rotation, ft
U	actual impeller speed at 7.00-inch radius (mean line), ft/sec
u	tangential velocity relative to impeller (positive in direction of rotation), ft/sec
v	through-flow component of velocity, ft/sec
W	total compressor flow rate, lb/sec
z	distance in axial direction

α angle between tangent to streamline in meridional plane and axis of rotation, deg

β blade angle (fig. 4, negative for backward-curved blades), deg

γ ratio of specific heats

δ ratio of total pressure at inlet to NACA standard sea-level pressure (29.92 in. Hg abs.)

η_{ad} adiabatic temperature-rise efficiency

θ ratio of inlet stagnation temperature to NACA standard sea-level temperature (518.4° R)

φ angle between projection of center line of blade inlet radial section and projection of center line of any other blade radial section on a plane perpendicular to axis of rotation (figs. 5 and 10), deg

φ' angle between projection of center line of blade inlet radial section and projection of radial line through driving face of splitter vane at hub on a plane perpendicular to axis of rotation (fig. 10), deg

λ prerotation term equal to $r_i(\omega r_i + u_i)$

ρ mass density, lb-sec^2/ft^4

ω angular velocity of impeller, radians/sec

Subscripts:

a average

d pressure or driving face of blade

e outlet conditions

i inlet conditions

s suction or trailing face of blade

t total

θ tangential component

APPENDIX B

METHOD OF EVALUATING BLADE SURFACE VELOCITIES

From appendix C of reference 5,

$$F_\theta = v\left(\frac{du}{dm} + \frac{u}{r}\sin\alpha + 2\omega\sin\alpha\right)$$

where F_θ is the blade force per unit mass in the tangential direction. Substituting $v = q\cos\beta$, $u = q\sin\beta$, and $dm = \frac{dz}{\cos\alpha}$ gives

$$F_\theta = q\cos\beta\left(\frac{du}{dz}\cos\alpha + \frac{q\sin\beta\sin\alpha}{r} + 2\omega\sin\alpha\right) \tag{B1}$$

$F_\theta\,\rho$ is the blade force per unit volume, which when multiplied by the circumferential distance between the blades gives the blade force per unit area or the pressure difference between the blades; thus,

$$F_\theta\,\rho\left(\frac{2\pi rf}{N}\right) = \Delta p \tag{B2}$$

Substituting equation (B1) in equation (B2) gives

$$\Delta p = \rho q\cos\beta\left(\frac{2\pi rf}{N}\right)\left(\frac{du}{dz}\cos\alpha + \frac{q\sin\beta\sin\alpha}{r} + 2\omega\sin\alpha\right) \tag{B3}$$

Assuming a linear variation of pressure from blade to blade yields

$$p_s = p_a - \frac{\Delta p}{2}$$

$$p_d = p_a + \frac{\Delta p}{2}$$

Dividing by total pressure P_i upstream of the impeller inlet gives

$$\frac{p_s}{P_i} = \frac{p_a}{P_i} - \frac{\Delta p}{2P_i} \tag{B4}$$

and

$$\frac{p_d}{P_i} = \frac{p_a}{P_i} + \frac{\Delta p}{2P_i} \tag{B5}$$

Equation (11) of reference 5 is

$$\rho = \rho_{t,i} \left\{ 1 + \frac{\gamma-1}{2} \left[\left(\frac{\omega r}{c_i} \right)^2 - \left(\frac{q}{c_i} \right)^2 \right] - \frac{\omega \lambda}{gJH_i} \right\}^{\frac{1}{\gamma-1}}$$

For zero prerotation at the inlet ($\lambda = 0$) and with

$$\frac{\rho}{\rho_{t,i}} = \left(\frac{p}{P_i} \right)^{\frac{1}{\gamma}}$$

The expression for velocity becomes

$$q^2 = (\omega r)^2 + \frac{2(c_i)^2}{\gamma-1} \left[1 - \left(\frac{p}{P_i} \right)^{\frac{\gamma-1}{\gamma}} \right] \tag{B6}$$

Substituting equations (B4) and (B5) in equation (B6) gives the final equations for determining the velocity on the blade surfaces,

$$q_s = \sqrt{(\omega r)^2 + \frac{2(c_i)^2}{\gamma-1} \left[1 - \left(\frac{p_a}{P_i} - \frac{\Delta p}{2P_i} \right)^{\frac{\gamma-1}{\gamma}} \right]} \tag{B7a}$$

and

$$q_d = \sqrt{(\omega r)^2 + \frac{2(c_i)^2}{\gamma-1} \left[1 - \left(\frac{p_a}{P_i} + \frac{\Delta p}{2P_i} \right)^{\frac{\gamma-1}{\gamma}} \right]} \tag{B7b}$$

REFERENCES

1. Goldstein, Arthur W., and Mager, Artur: Attainable Circulation About Airfoils in Cascade. NACA Rep. 953, 1950. (Supersedes NACA TN 1941.)

2. Michel, Donald J., Ginsburg, Ambrose, and Mizisin, John: Experimental Investigation of Flow in the Rotating Passages of a 48-Inch Impeller at Low Tip Speeds. NACA RM E51D20, 1951.

3. Michel, Donald J., Mizisin, John, and Prian, Vasily D.: Effect of Changing Passage Configuration upon Internal-Flow Characteristics of a 48-Inch Centrifugal Compressor. I - Change in Blade Shape. NACA TN 2706, 1952.

4. Stanitz, John D.: Approximate Design Method for High-Solidity Blade Elements in Compressors and Turbines. NACA TN 2408, 1951.

5. Hamrick, Joseph T., Ginsburg, Ambrose, and Osborn, Walter M.: Method of Analysis for Compressible Flow Through Mixed-Flow Centrifugal Impellers of Arbitrary Design. NACA TN 2165, 1950.

6. Withee, Joseph R., Jr., and Beede, William L.: Design and Test of Mixed Flow Impellers. II - Experimental Results, Impeller Model MFI-1A. NACA RM E52E22, 1952.

[redacted]

TABLE I - GEOMETRIC COORDINATES OF MFI-1 AND MFI-1A IMPELLERS[a]

Axial depth (in.)	Blade thickness at hub (in.)	Blade thickness at mean line, MFI-1 (in.)	Blade thickness at shroud, MFI-1A (in.)	Hub radius (in.)	Mean-line radius, MFI-1 (in.)	Shroud radius, MFI-1 (in.)	Shroud radius, MFI-1A (in.)	Angle φ (b)	Angle φ' (c)
0	0.062	0.022	0.022	1.678	3.210	4.725	4.725	0°	------
.200	.065	.024	.024	1.695	3.252	4.736	4.763	3°24'	------
.400	.090	.048	.048	1.718	3.308	4.758	4.792	6°41'	------
.600	.165	.122	.084	1.752	3.384	4.789	4.819	9°46'	------
.800	.237	.193	.121	1.801	3.490	4.823	4.863	12°40'	------
1.000	.260	.260	.192	1.864	3.619	4.868	4.915	15°06'	------
1.400	.296	.296	.236	2.050	3.900	4.973	5.040	18°38'	------
1.800	.288	.288	.235	2.360	4.180	5.098	5.200	20°54'	------
2.200	.272	.272	.223	2.985	4.448	5.247	5.380	22°18'	------
2.600	.264	.264	.218	3.704	4.708	5.417	5.580	23°06'	------
3.000	.260	.260	.217	4.120	4.964	5.611	5.782	23°29'	------
3.400	.298	.259	.218	4.476	5.220	5.808	6.006	23°37'	------
3.625	----	----	----	-----	-----	-----	-----	------	15°05'
3.800	.291	.257	.218	4.812	5.472	6.005	6.228	23°39'	15°05'
4.200	.283	.252	.214	5.138	5.724	6.203	6.454	23°31'	14°57'
4.600	.267	.240	.203	5.456	5.978	6.399	6.680	23°24'	14°50'
5.000	.244	.220	.185	5.764	6.228	6.598	6.902	23°21'	14°47'
5.400	.208	.186	.152	6.056	6.480	6.795	7.128	23°23'	14°49'
5.800	.147	.128	.095	6.349	6.716	6.992	7.352	23°29'	14°55'
6.200	.060	.044	.044	6.634	6.940	7.190	7.580	23°55'	15°21'
6.310	.025	.010	.010	6.710	7.000	7.247	7.644	24°05'	15°31'

[a] Splitter-blade thickness at hub is 0.120 in. and at shroud 0.060 in.; leading edge is cut back from z = 3.625 in. at hub along line making a 30° angle with radius through z = 3.625 in. (see fig. 11); number of blades, 21; material used for construction of impeller was aluminum (14S-T6).

[b] See figure 5 and appendix A.

[c] See figure 10 and appendix A.

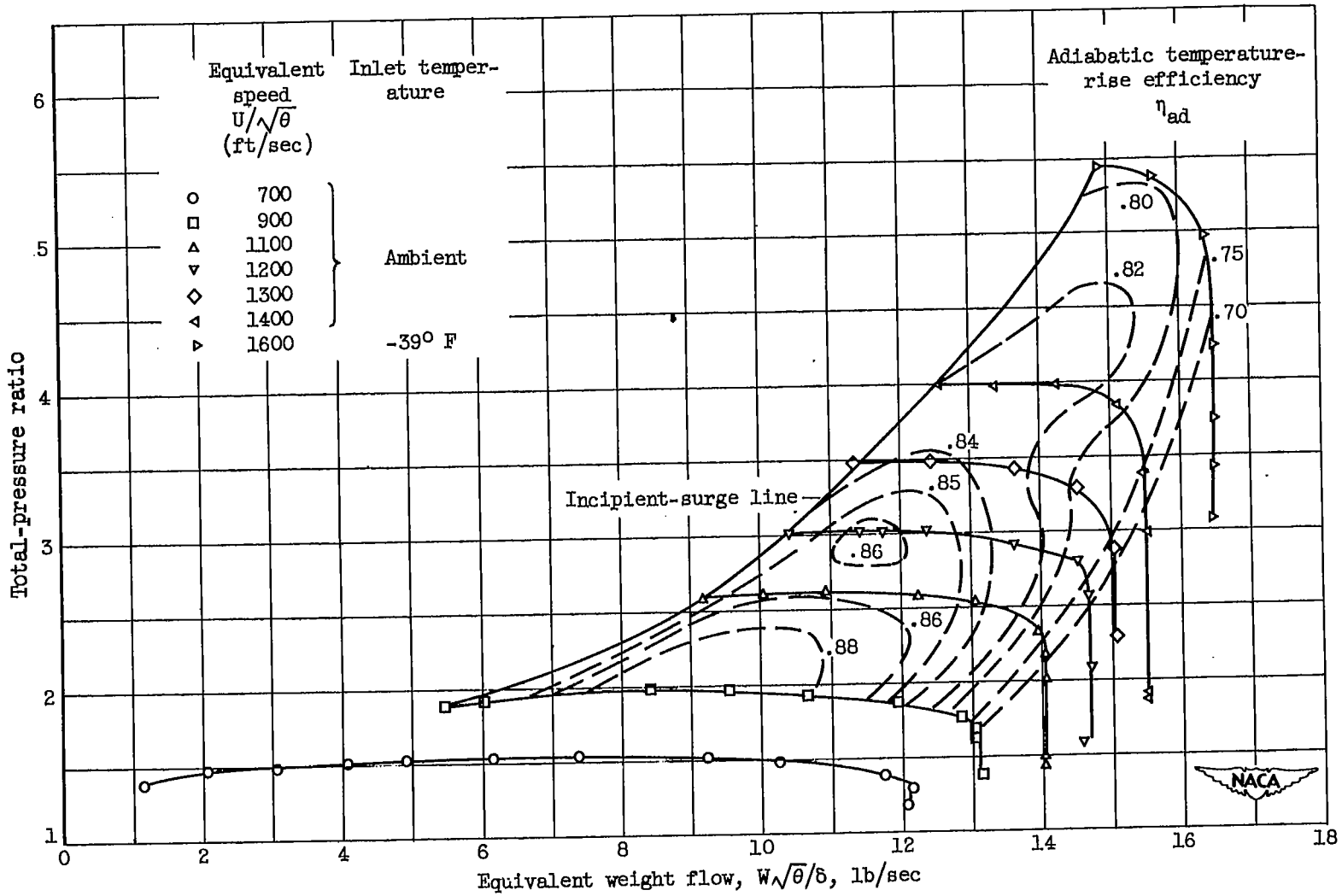

Figure 1. - Performance characteristics for modified impeller (MFI-1A) (reference 6).

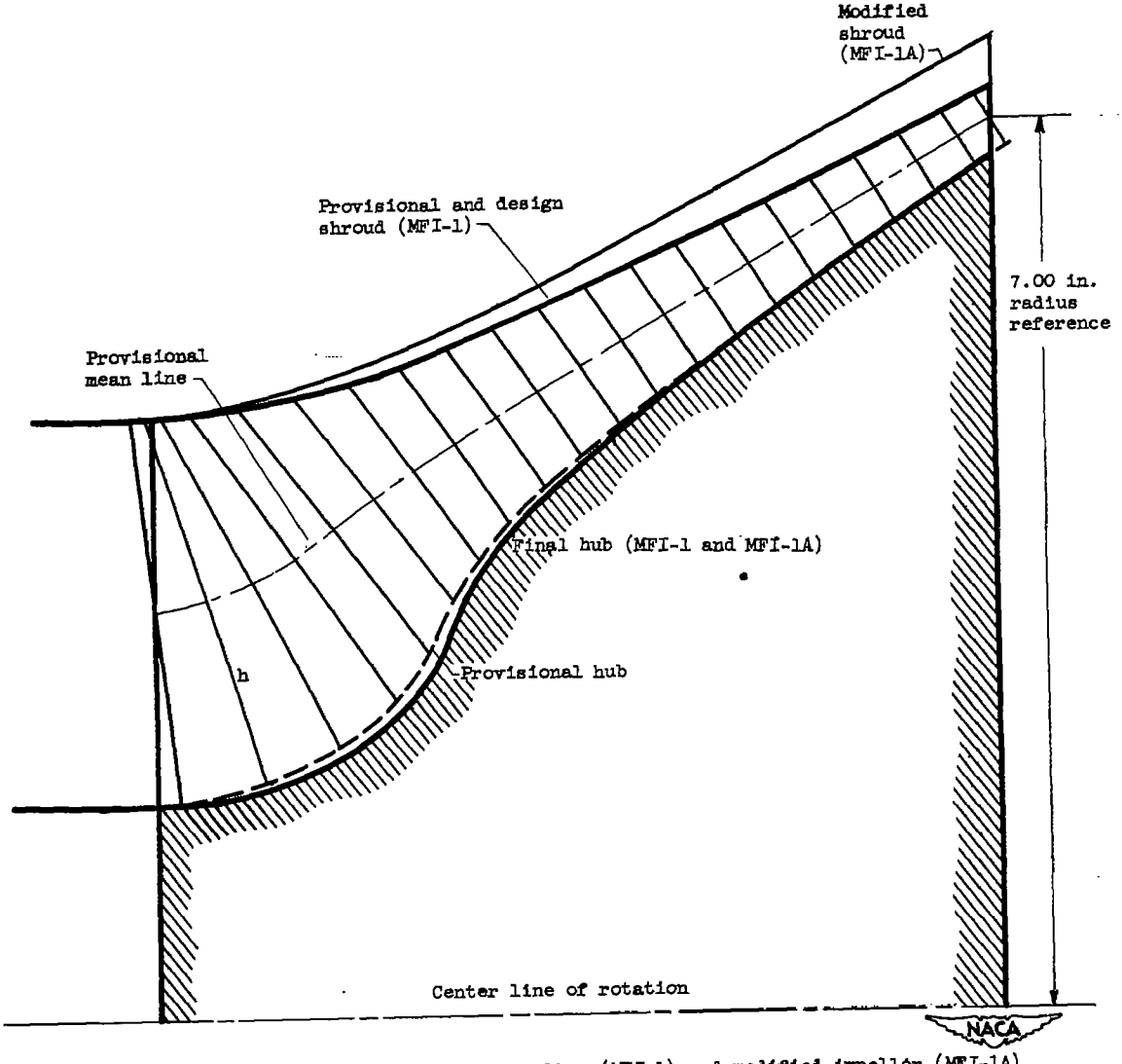

Figure 2. - Hub-shroud profile of design impeller (MFI-1) and modified impeller (MFI-1A).

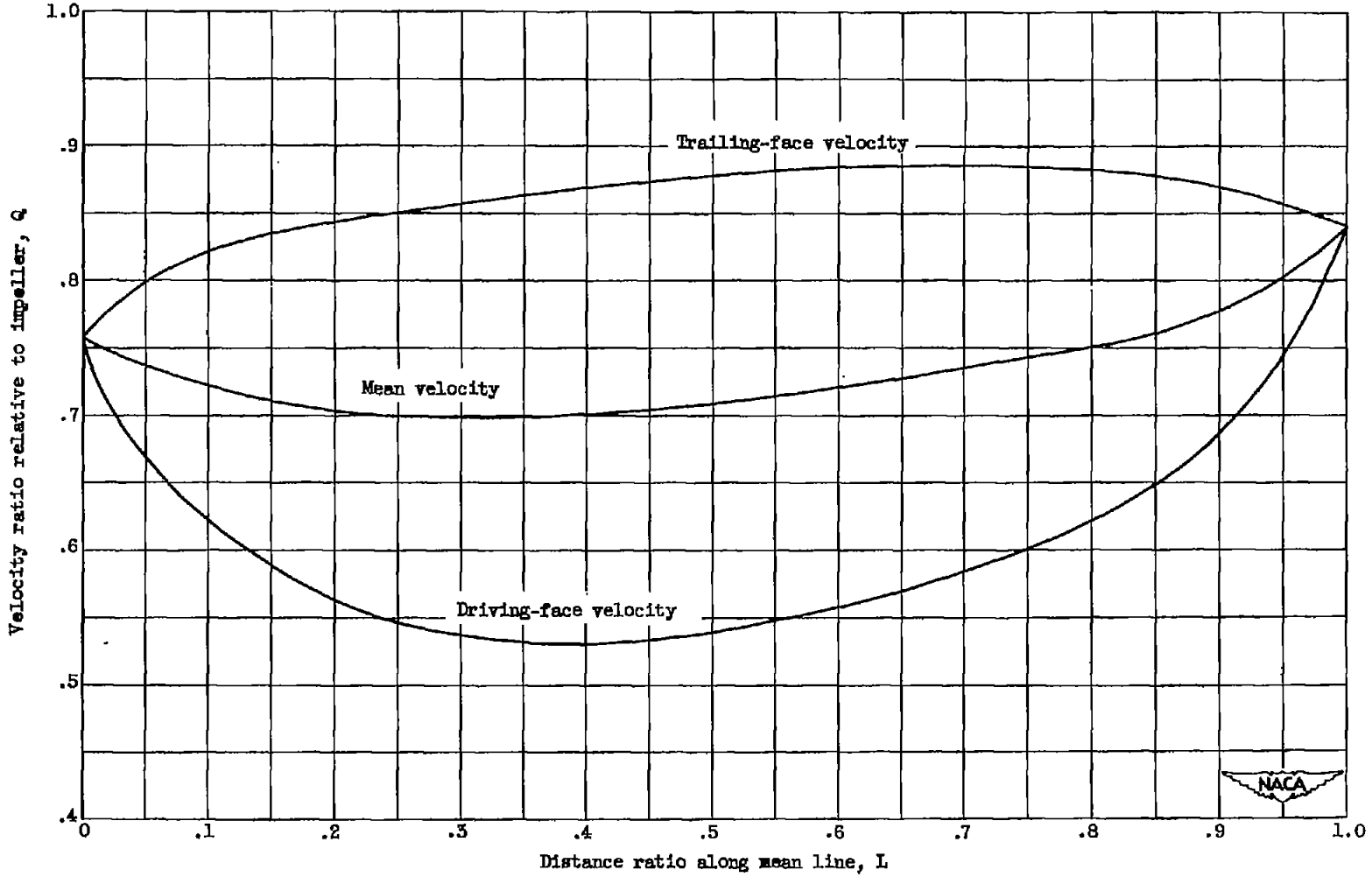

Figure 3. - Prescribed velocity diagram for design impeller (MFI-1).

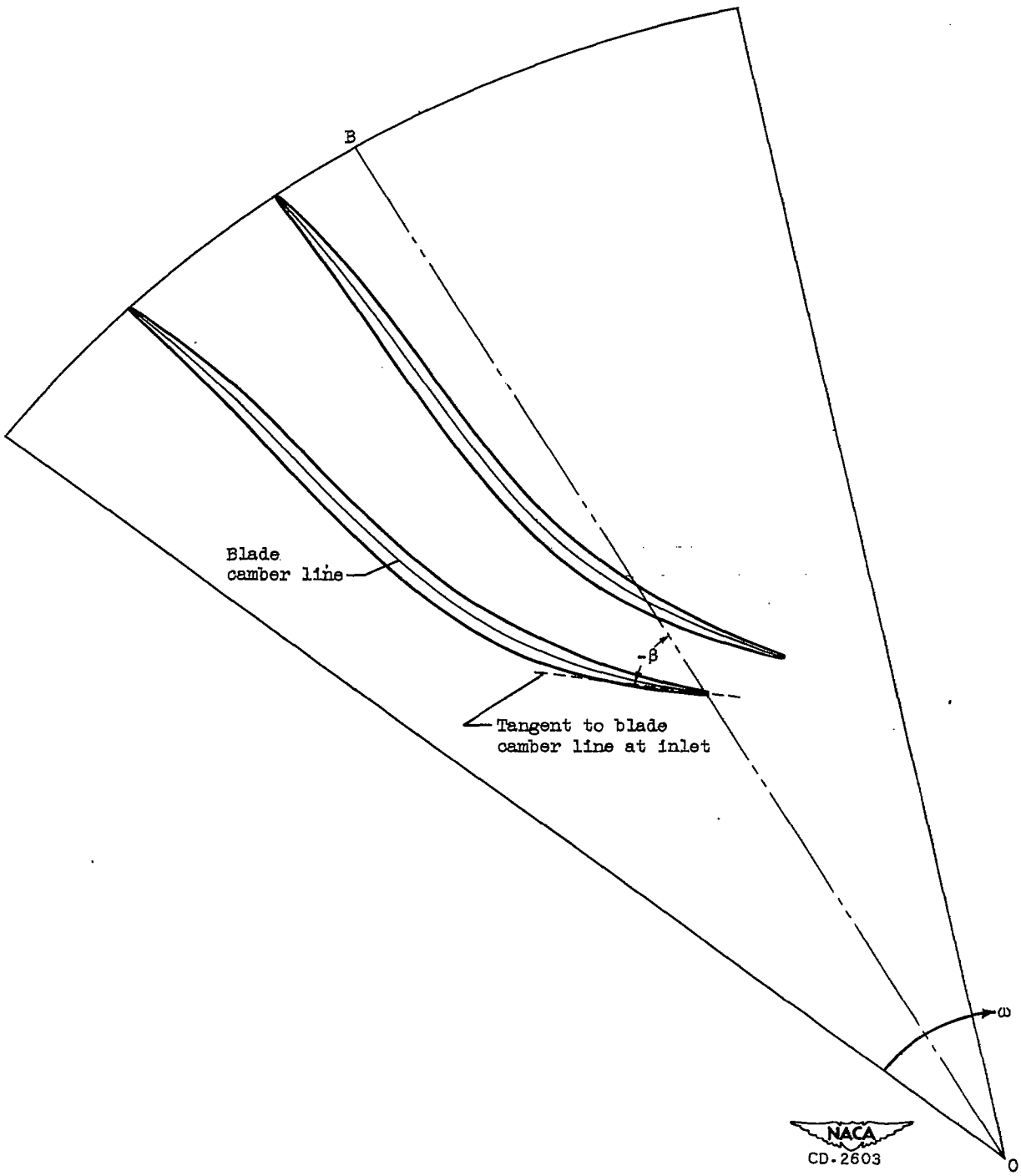

Figure 4. - Impeller passage on developed cone surface showing orientation of blade angle β and design blade shape.

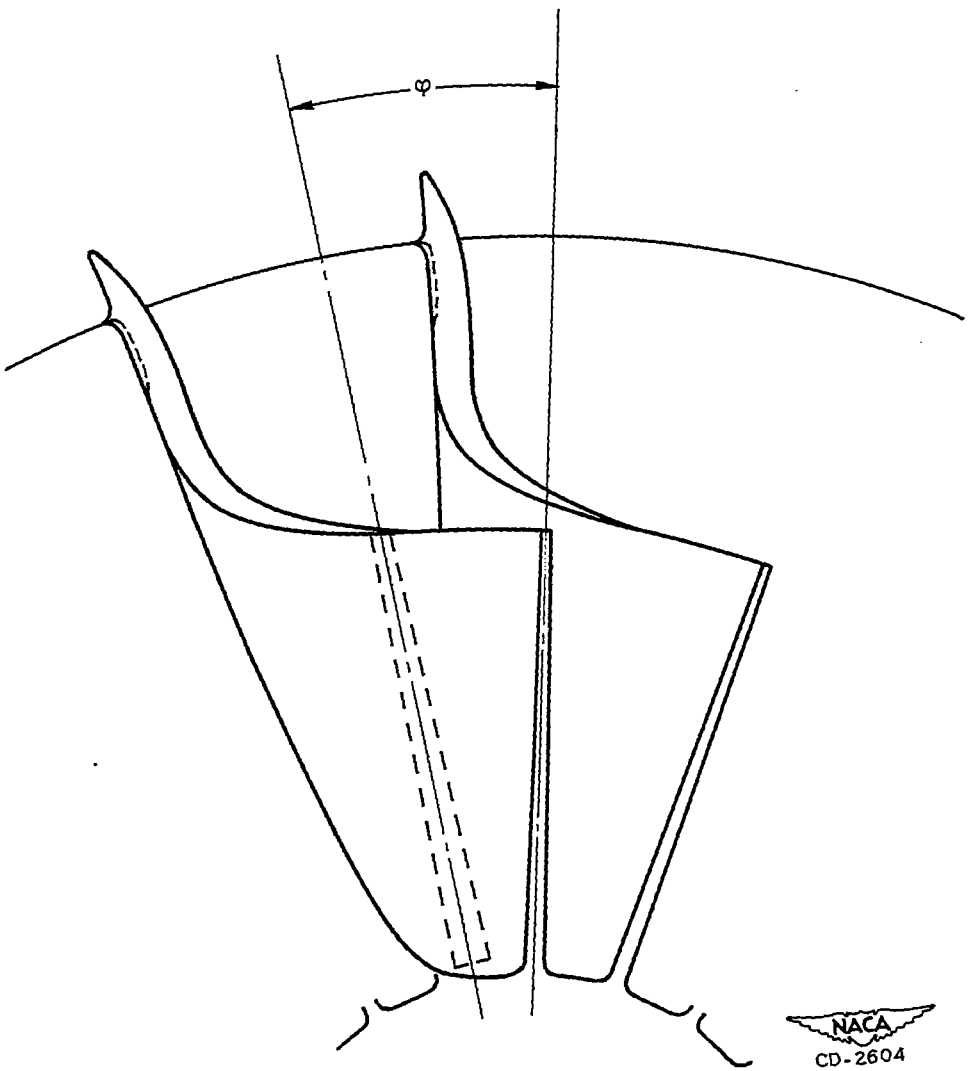

Figure 5. - Front view of design impeller (MFI-1) showing orientation of angle φ.

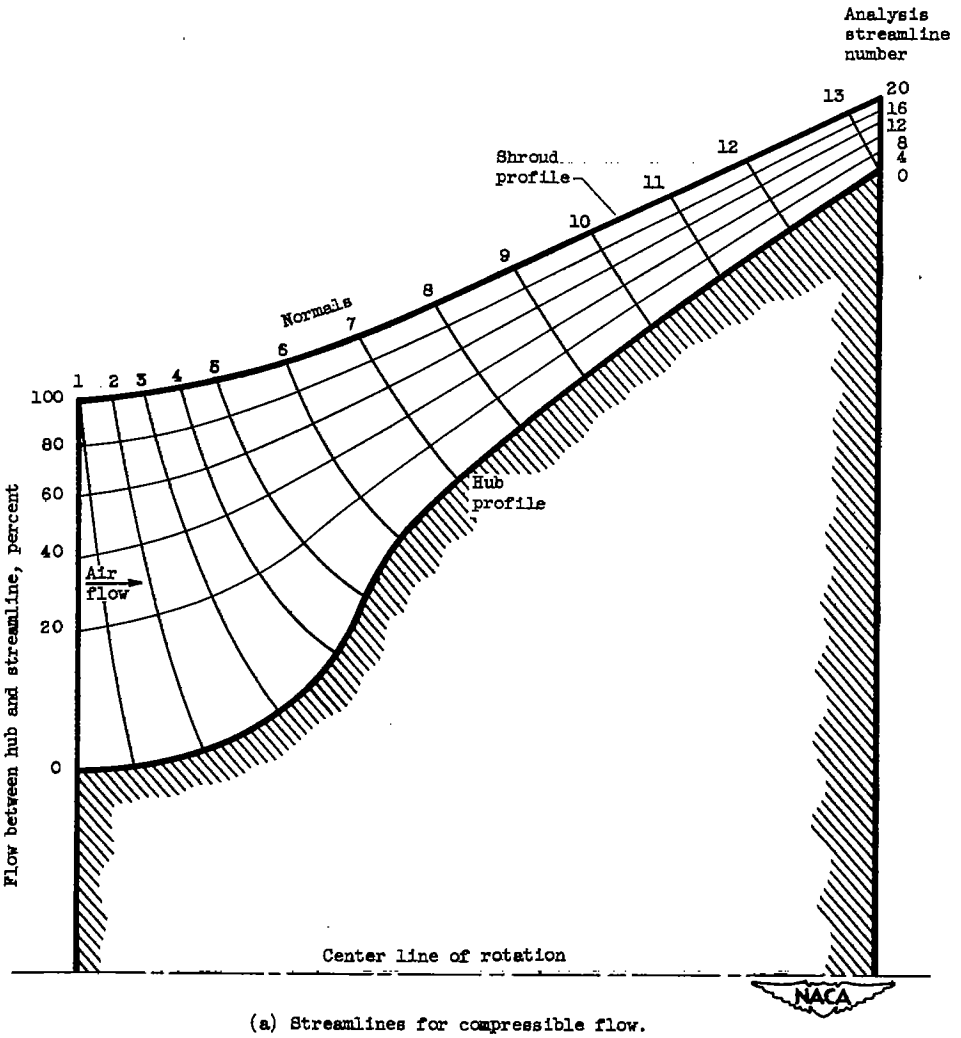

(a) Streamlines for compressible flow.

Figure 6. - Flow analysis for design impeller (MFI-1) in the meridional plane for weight flow of 14.5 pounds per second and outlet mean-line speed of 1400 feet per second.

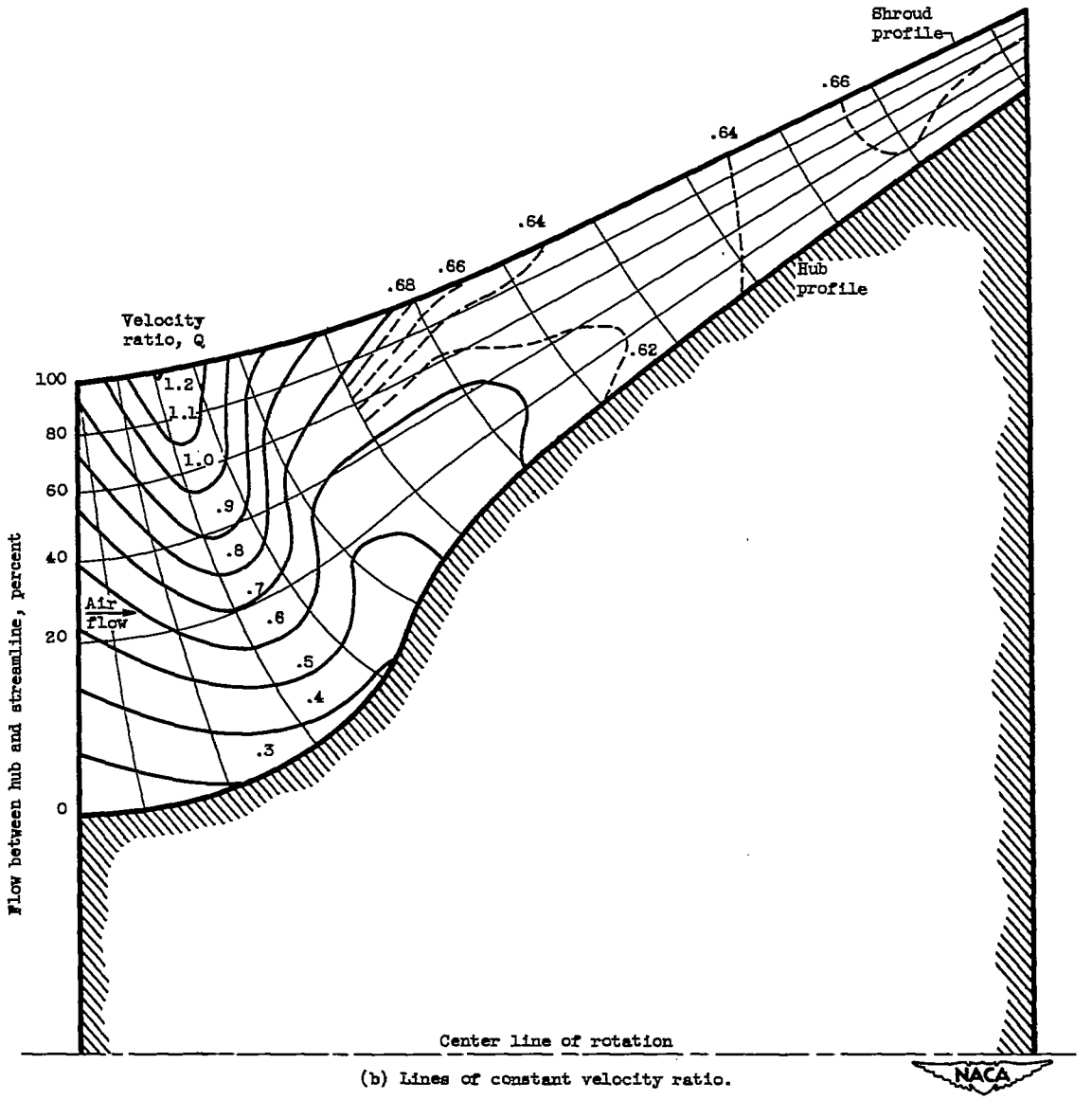

(b) Lines of constant velocity ratio.

Figure 6. - Continued. Flow analysis for design impeller (MFI-1) in meridional plane for weight flow of 14.5 pounds per second and outlet mean-line speed of 1400 feet per second.

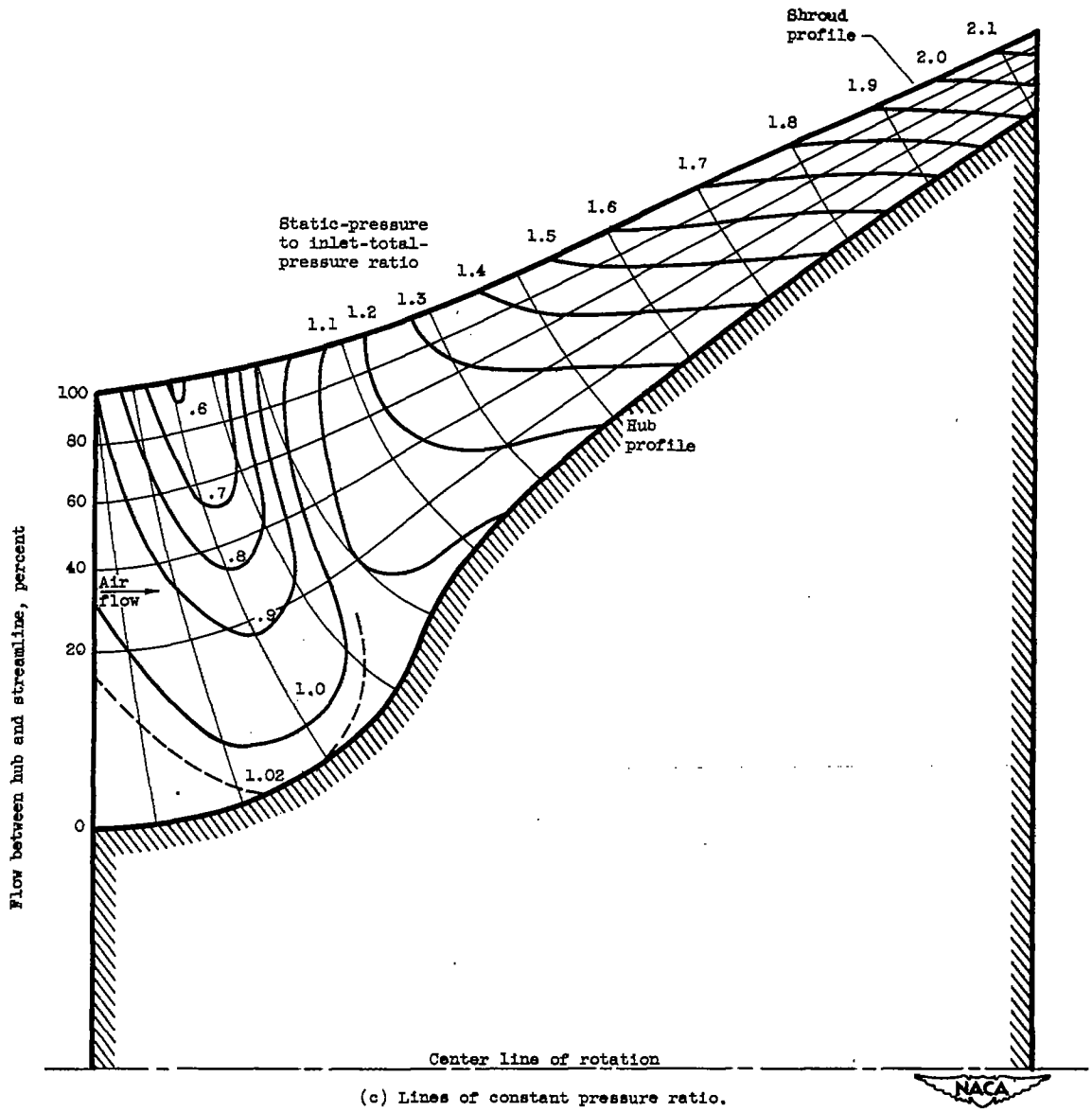

(c) Lines of constant pressure ratio.

Figure 6. - Concluded. Flow analysis for design impeller (MFI-1) in meridional plane for weight flow of 14.5 pounds per second and outlet mean-line speed of 1400 feet per second.

[redacted]

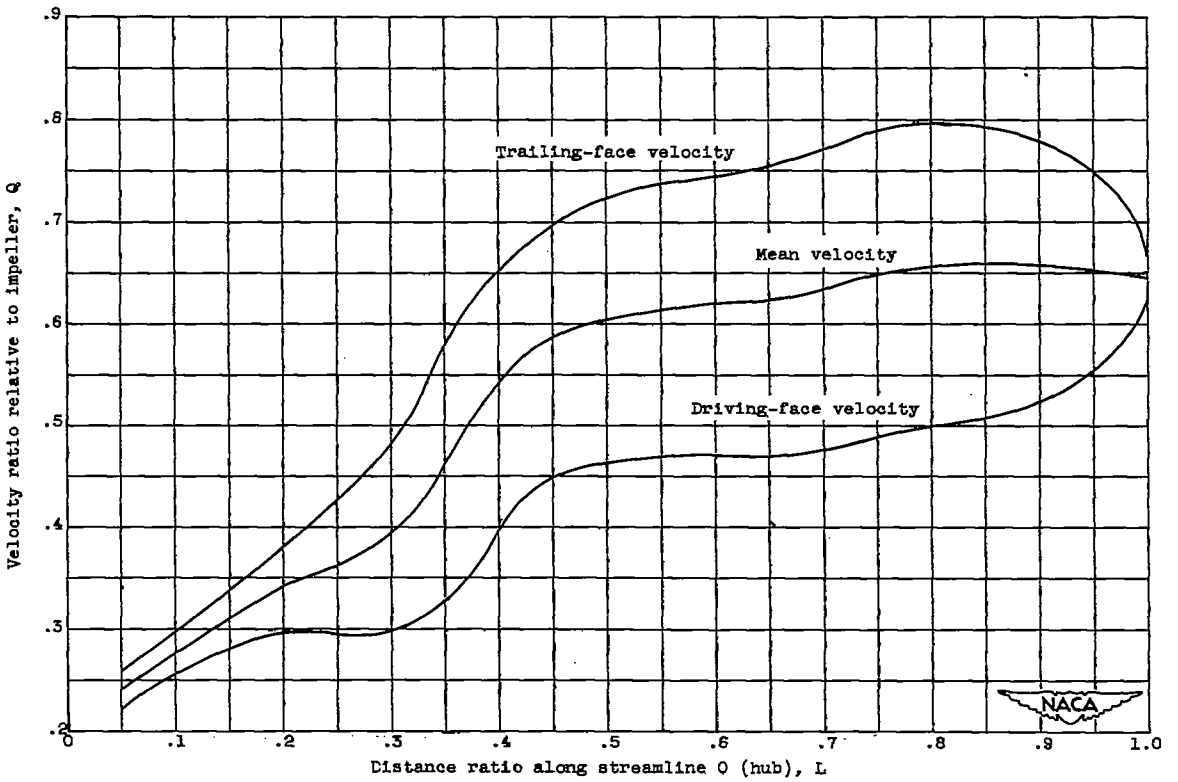

(a) Blade to blade velocity distribution along streamline 0 (hub).

Figure 7. - Flow analysis in blade to blade plane for design impeller (MFI-1) for weight flow of 14.5 pounds per second and outlet mean-line speed of 1400 feet per second.

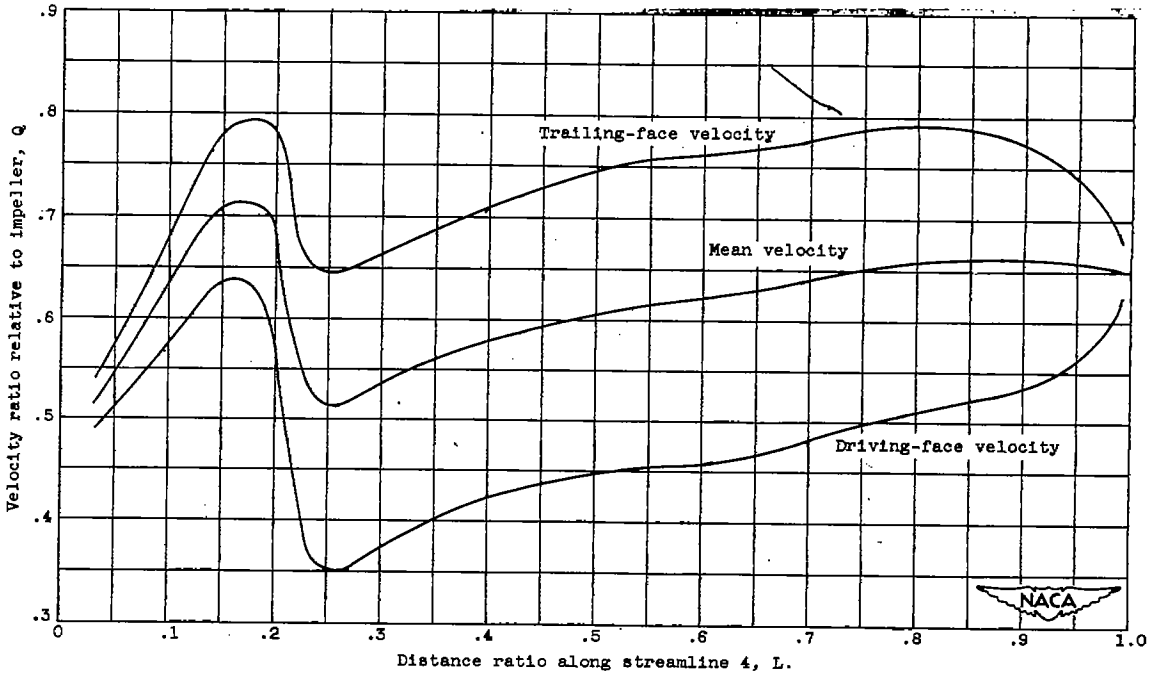

(b) Blade to blade velocity distribution along streamline 4.

Figure 7. - Continued. Flow analysis in blade to blade plane for design impeller (MFI-1) for weight flow of 14.5 pounds per second and outlet mean-line speed of 1400 feet per second.

[redacted]

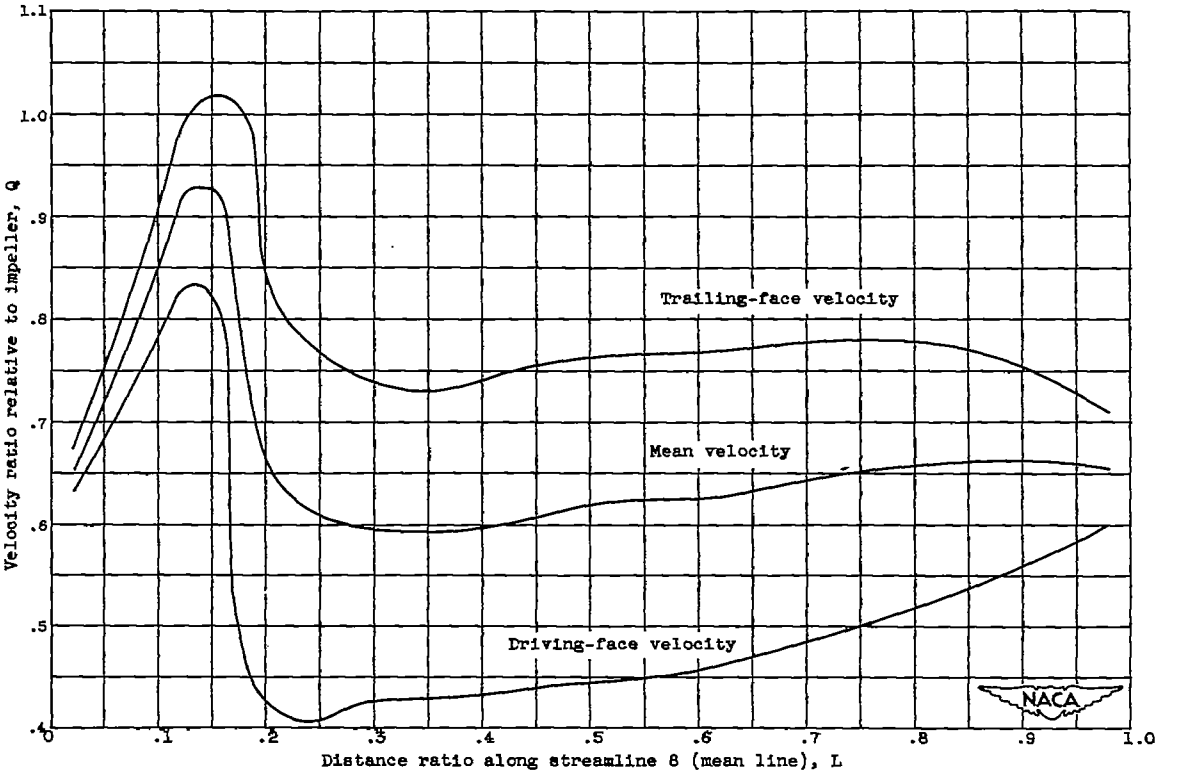

(c) Blade to blade velocity distribution along streamline 8 (mean line).

Figure 7. - Continued. Flow analysis in blade to blade plane for design impeller (MFI-1) for weight flow of 14.5 pounds per second and outlet mean-line speed of 1400 feet per second.

[redacted]

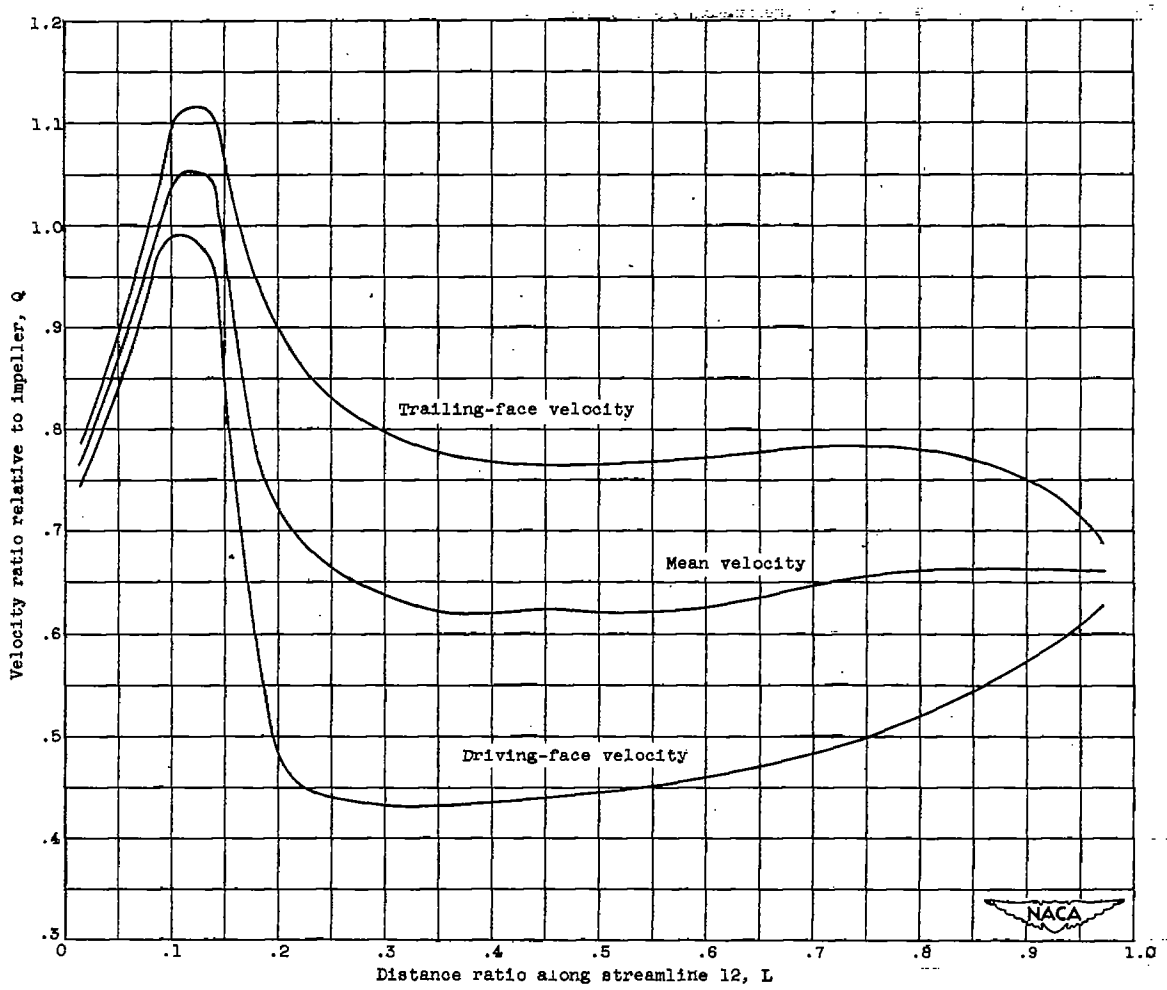

(d) Blade to blade velocity distribution along streamline 12.

Figure 7. - Continued. Flow analysis in blade to blade plane for design impeller (MFI-1) for weight flow of 14.5 pounds per second and outlet mean-line speed of 1400 feet per second.

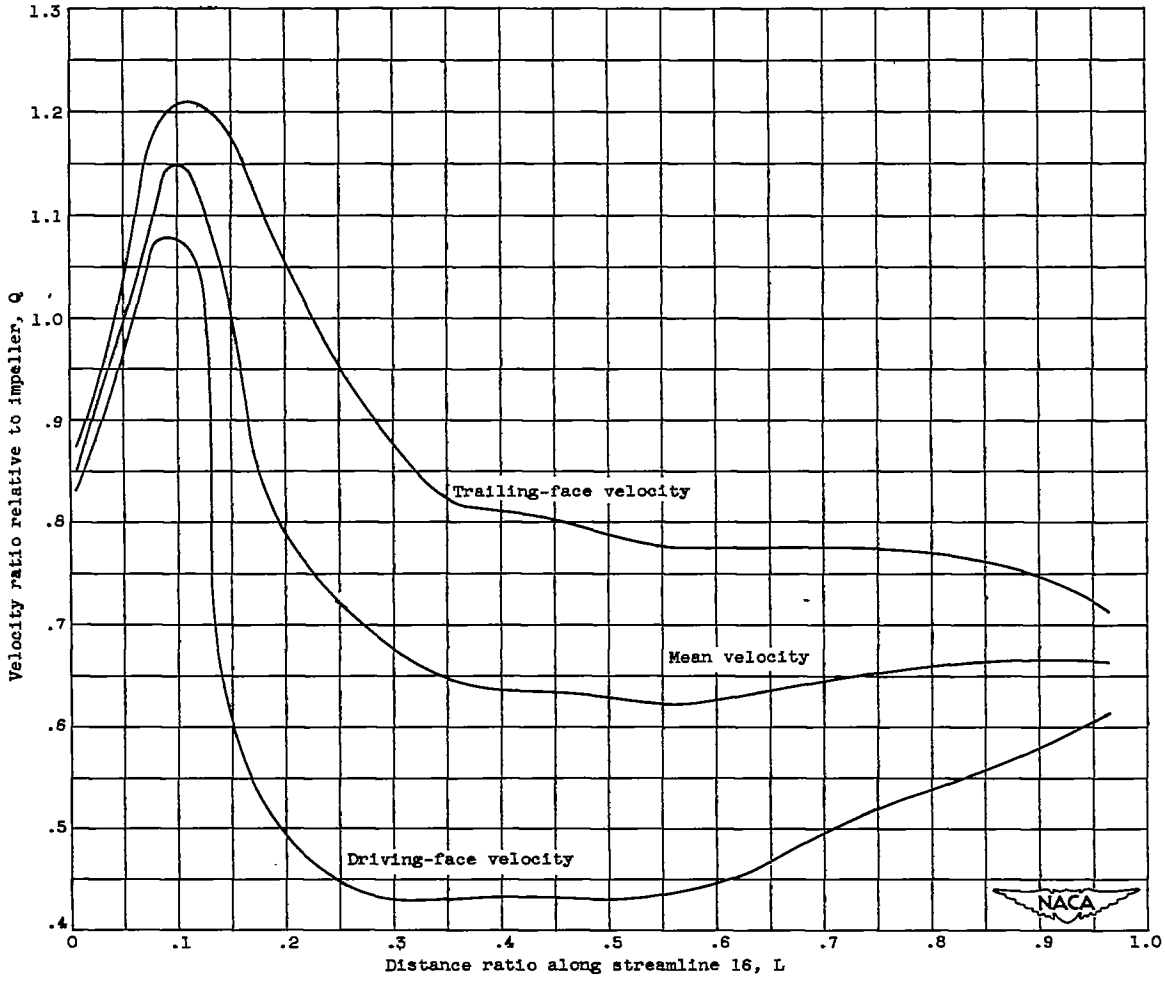

(e) Blade to blade velocity distribution along streamline 16.

Figure 7. - Continued. Flow analysis in blade to blade plane for design impeller (MFI-1) for weight flow of 14.5 pounds per second and outlet mean-line speed of 1400 feet per second.

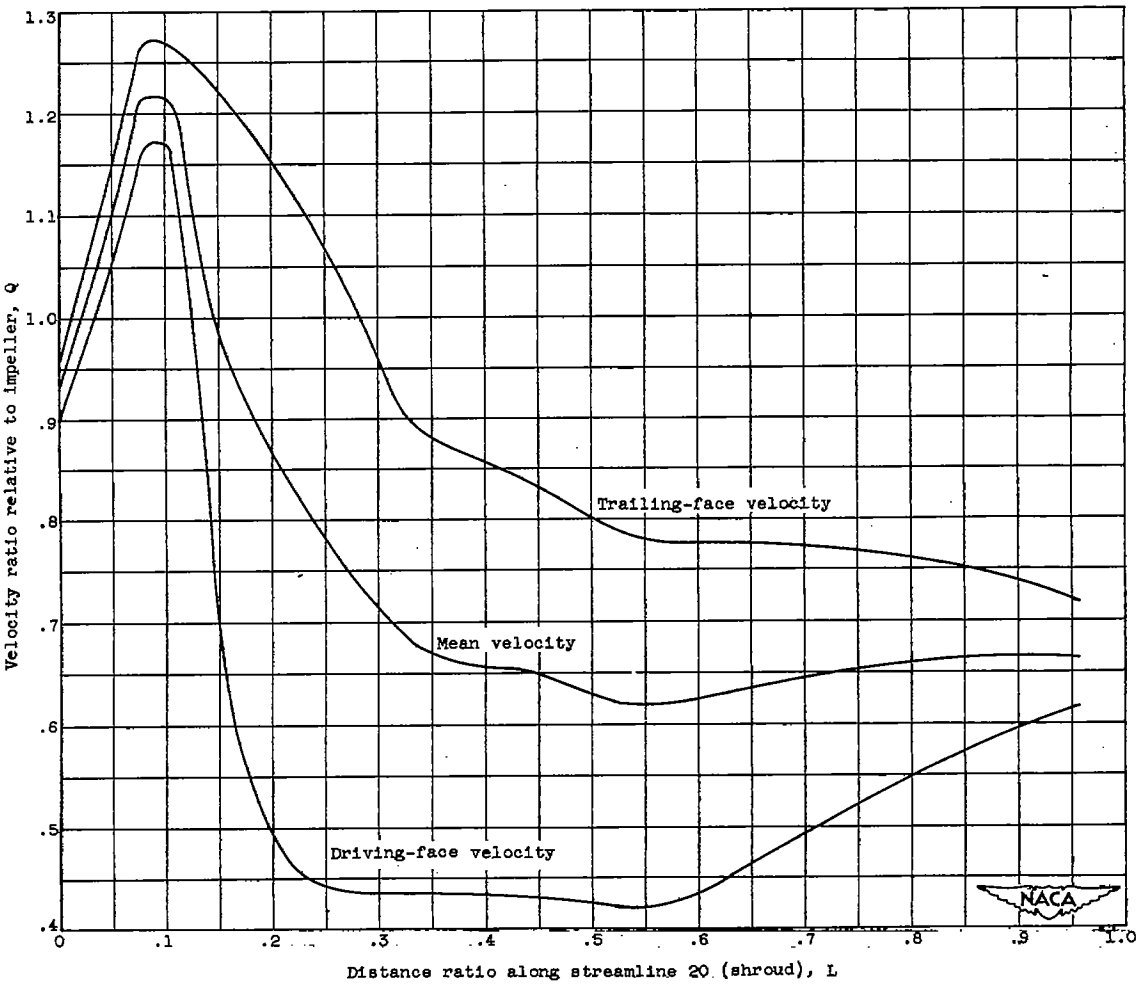

(f) Blade to blade velocity distribution along streamline 20 (shroud).

Figure 7. - Concluded. Flow analysis in blade to blade plane for design impeller (MFI-1) for weight flow of 14.5 pounds per second and outlet mean-line speed of 1400 feet per second.

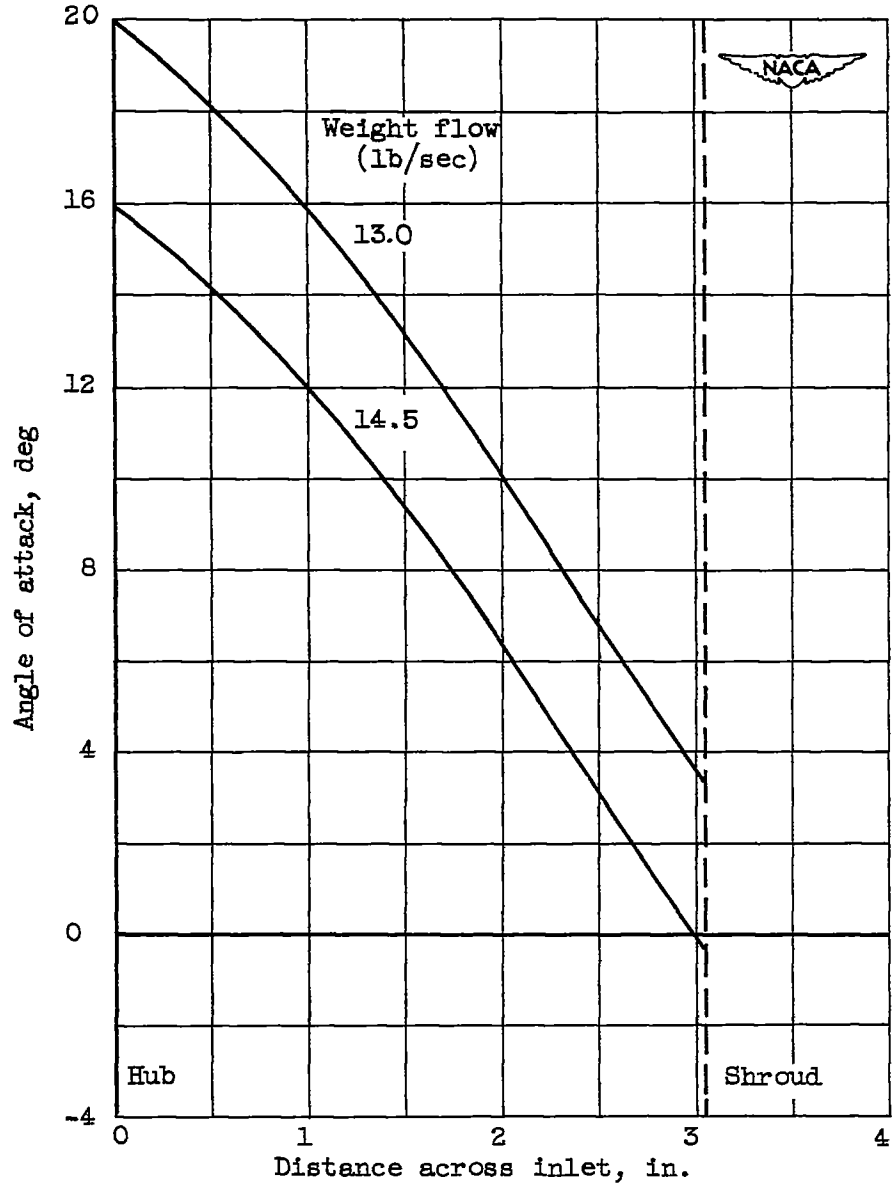

Figure 8. - Variation of theoretical angle of attack at inlet for MFI-1 and MFI-1A impellers.

[redacted]

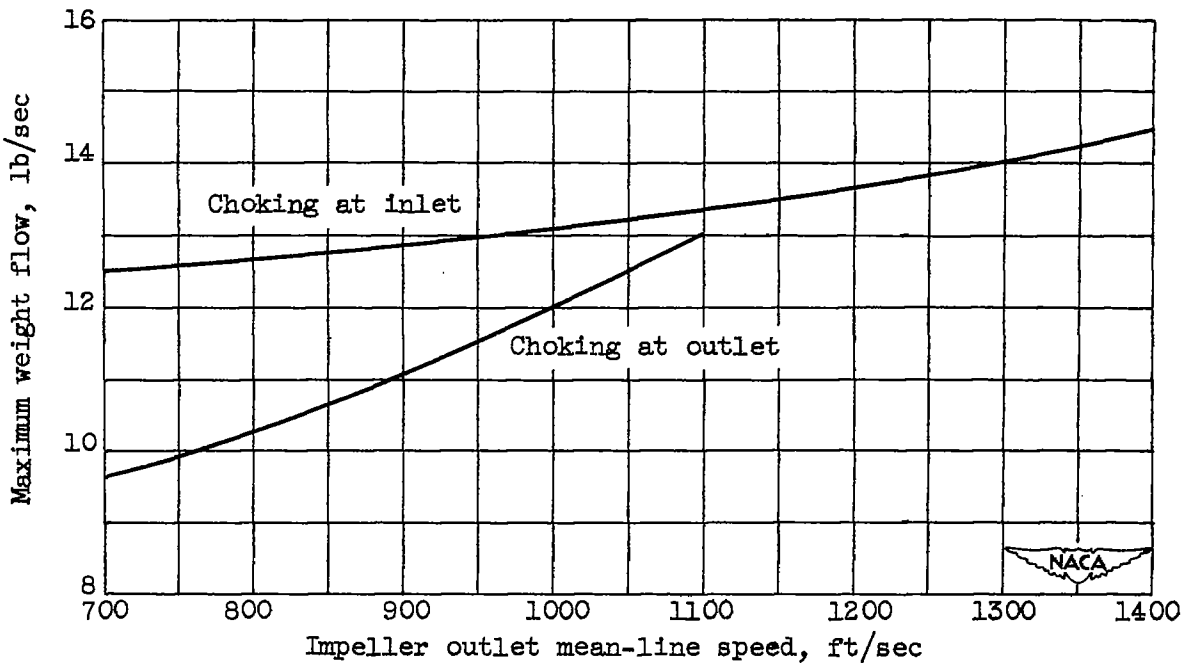

Figure 9. - Maximum weight flow for MFI-1 impeller.

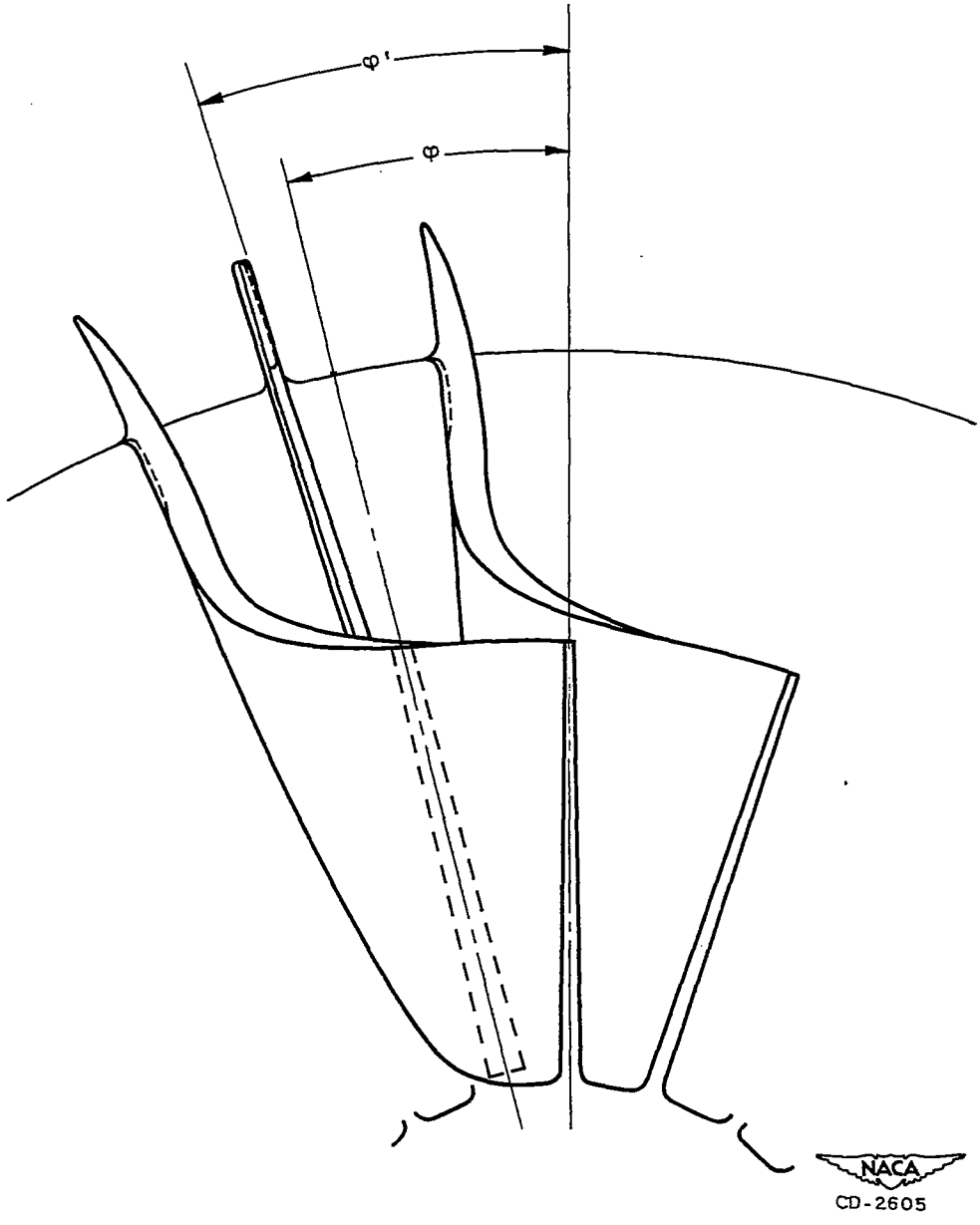

Figure 10. - Front view of modified impeller (MFI-1A) showing orientation of angles φ and φ'.

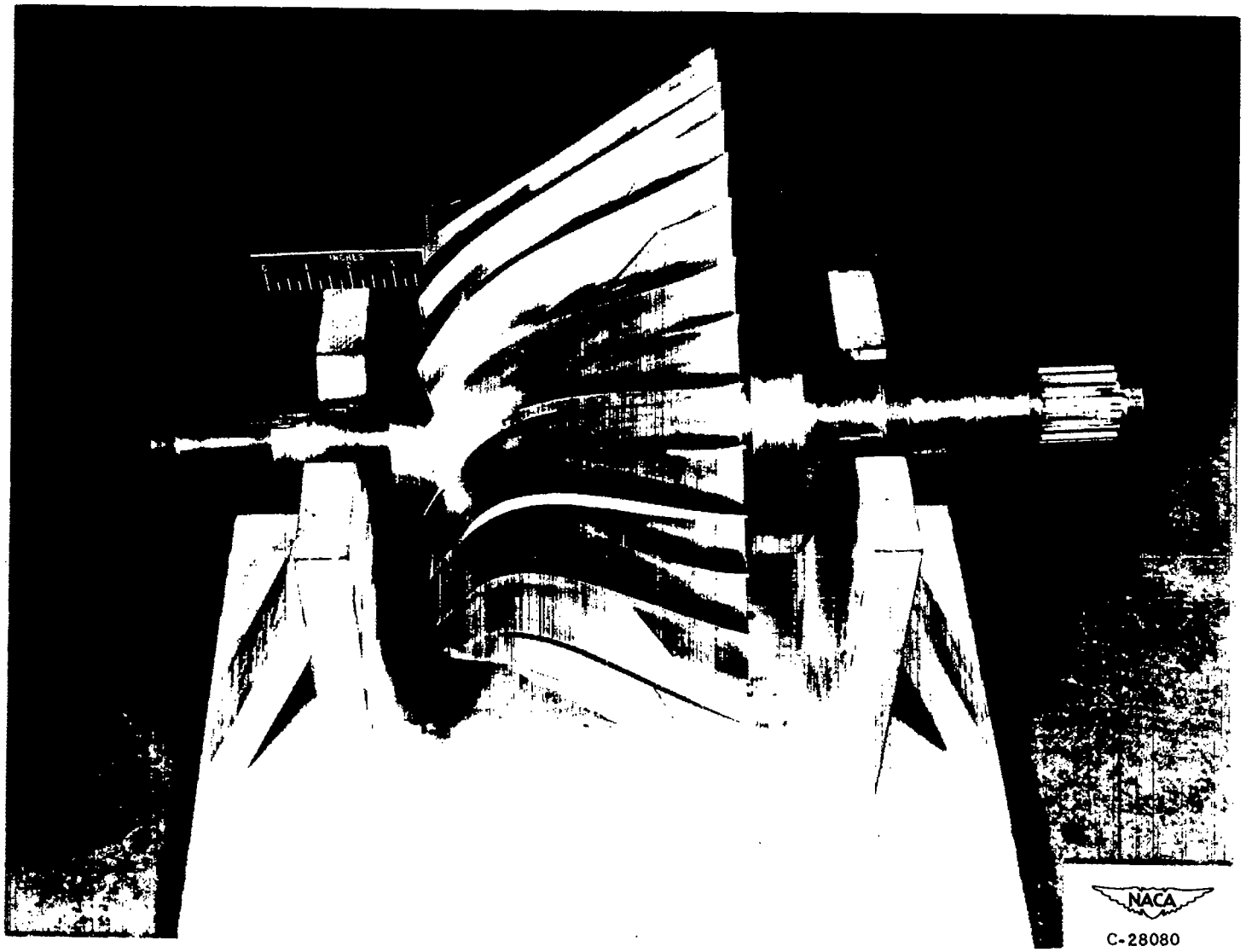

Figure 11. - Modified impeller (MFI-1A).

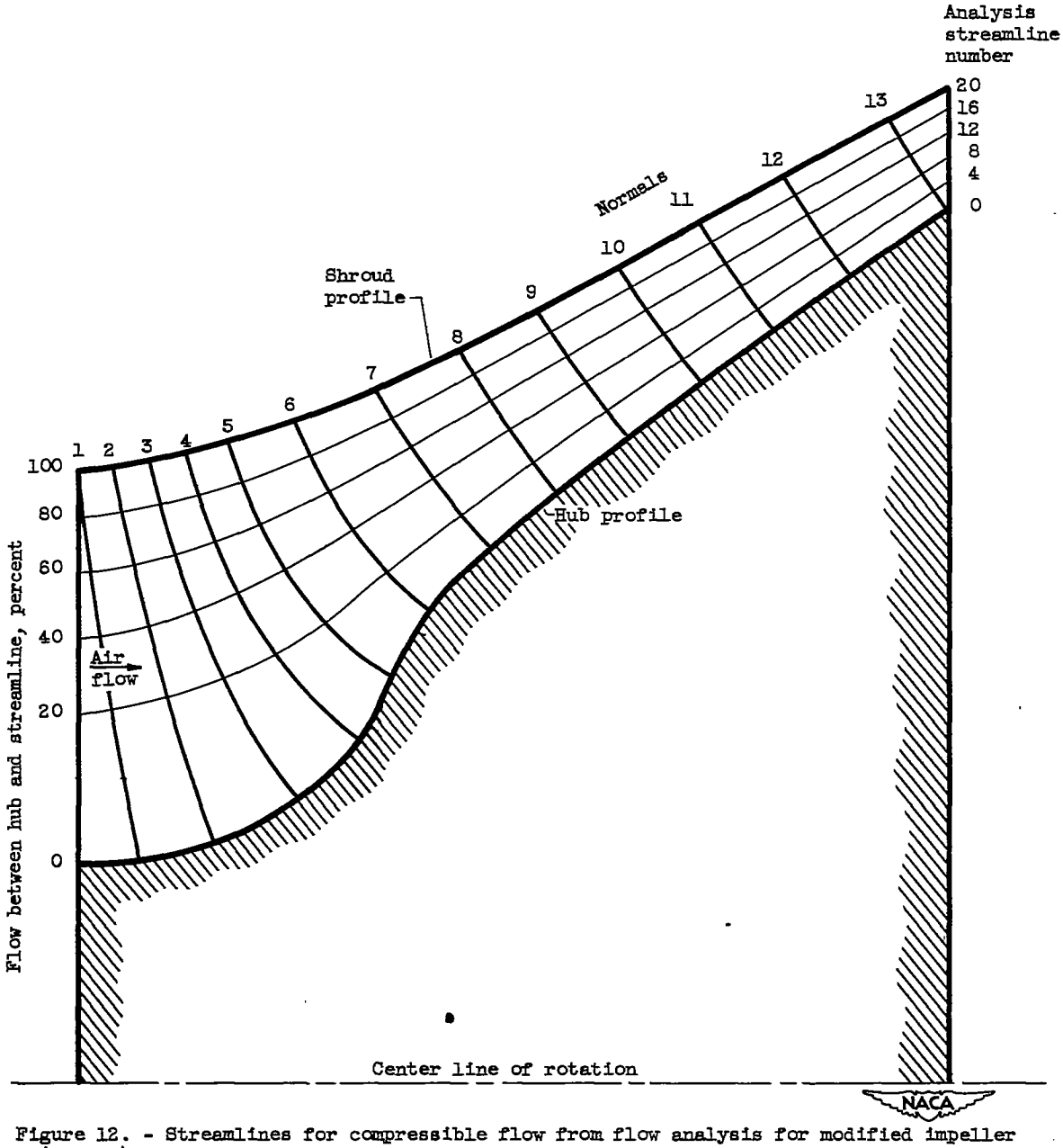

Figure 12. - Streamlines for compressible flow from flow analysis for modified impeller (MFI-1A) in meridional plane for weight flow of 13.0 pounds per second and outlet mean-line speed of 1400 feet per second.

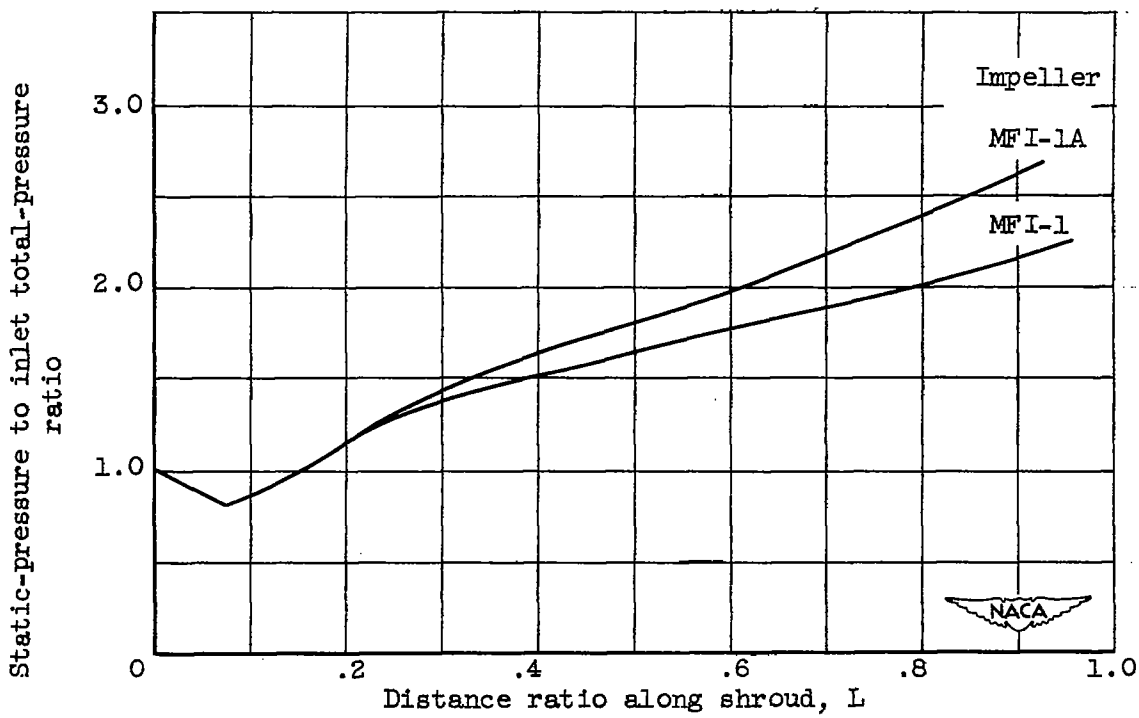

Figure 13. - Comparison of theoretical static-pressure for MFI-1 and MFI-1A impellers at weight flow of 13.0 pounds per second and outlet mean-line speed of 1400 feet per second.

[redacted]

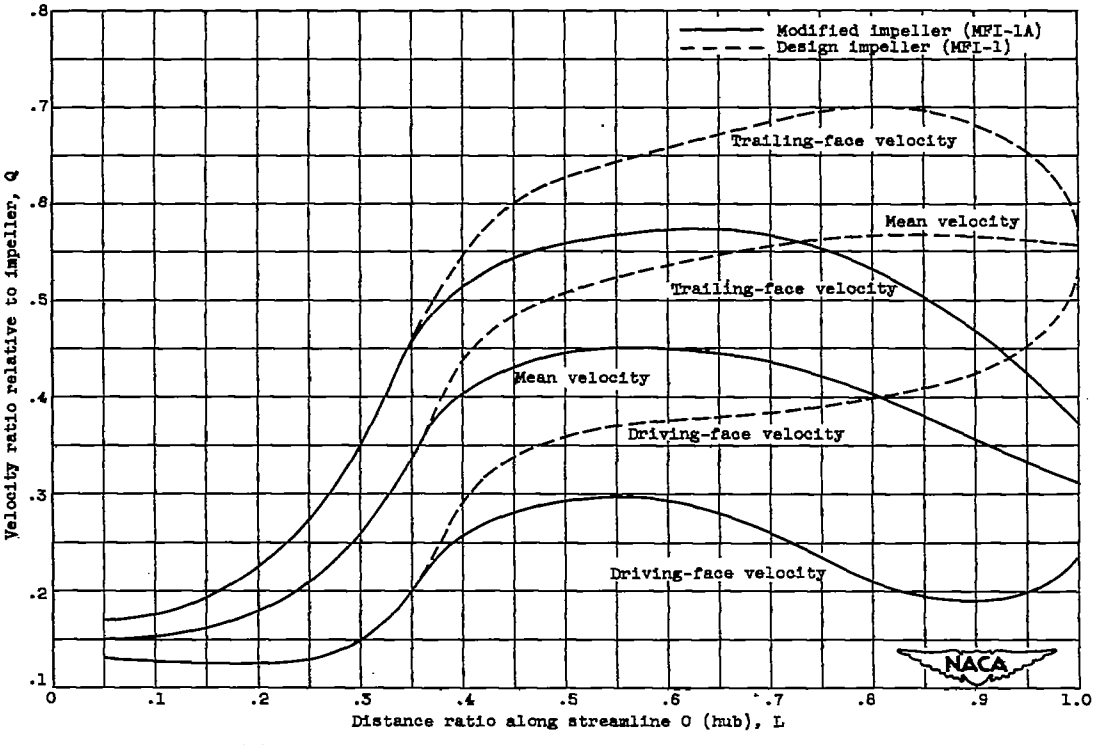

(a) Blade to blade velocity distribution along streamline O (hub).

Figure 14. - Flow analysis in blade to blade plane for MFI-1 and MFI-1A impellers for weight flow of 13.0 pounds per second and outlet mean-line speed of 1400 feet per second.

[redacted]

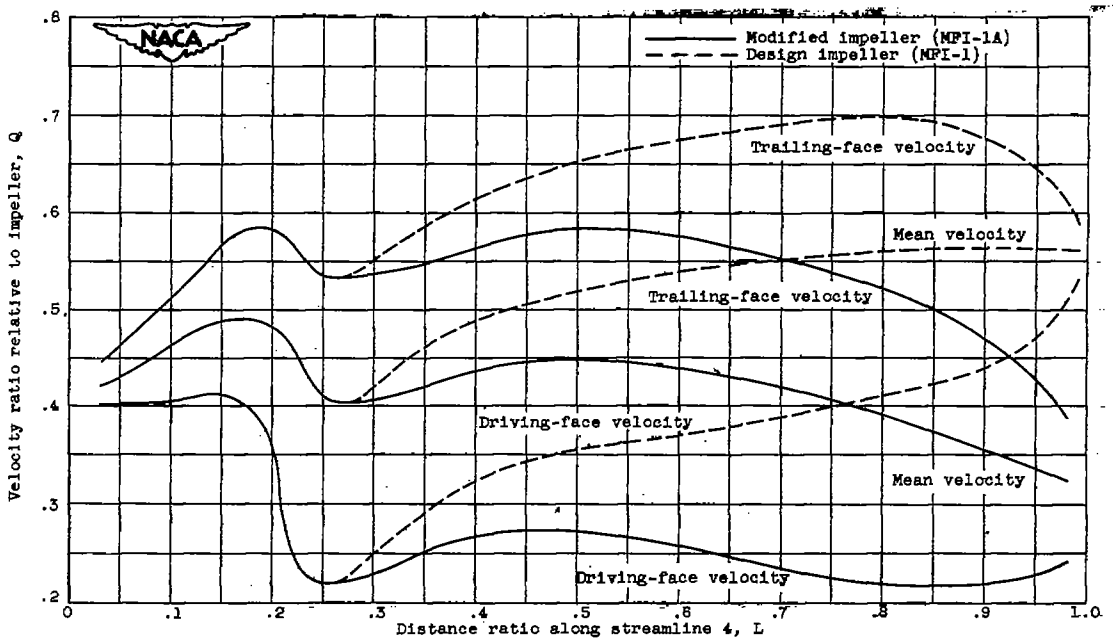

(b) Blade to blade velocity distribution along streamline 4.

Figure 14. - Continued. Flow analysis in blade to blade plane for MFI-1 and MFI-1A impellers for weight flow of 13.0 pounds per second and outlet mean-line speed of 1400 feet per second.

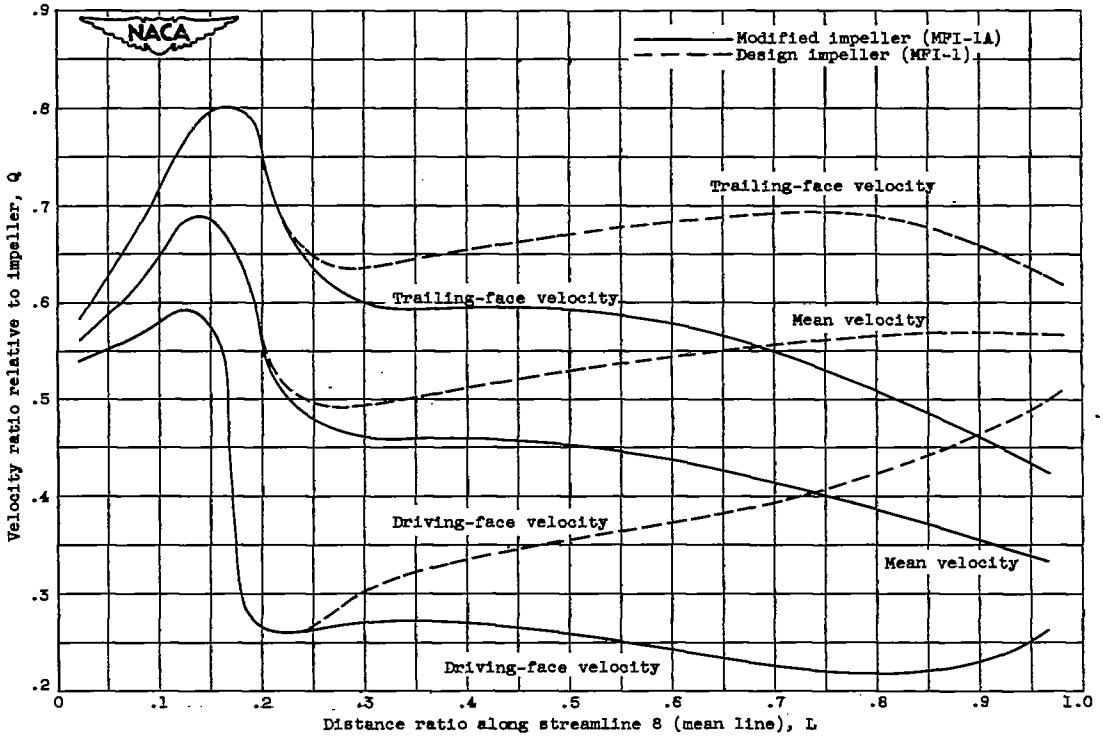

(c) Blade to blade velocity distribution along streamline S (mean line).

Figure 14. - Continued. Flow analysis in blade to blade plane for MFI-1 and MFI-1A impellers for weight flow of 15.0 pounds per second and outlet mean-line speed of 1400 feet per second.

[redacted]

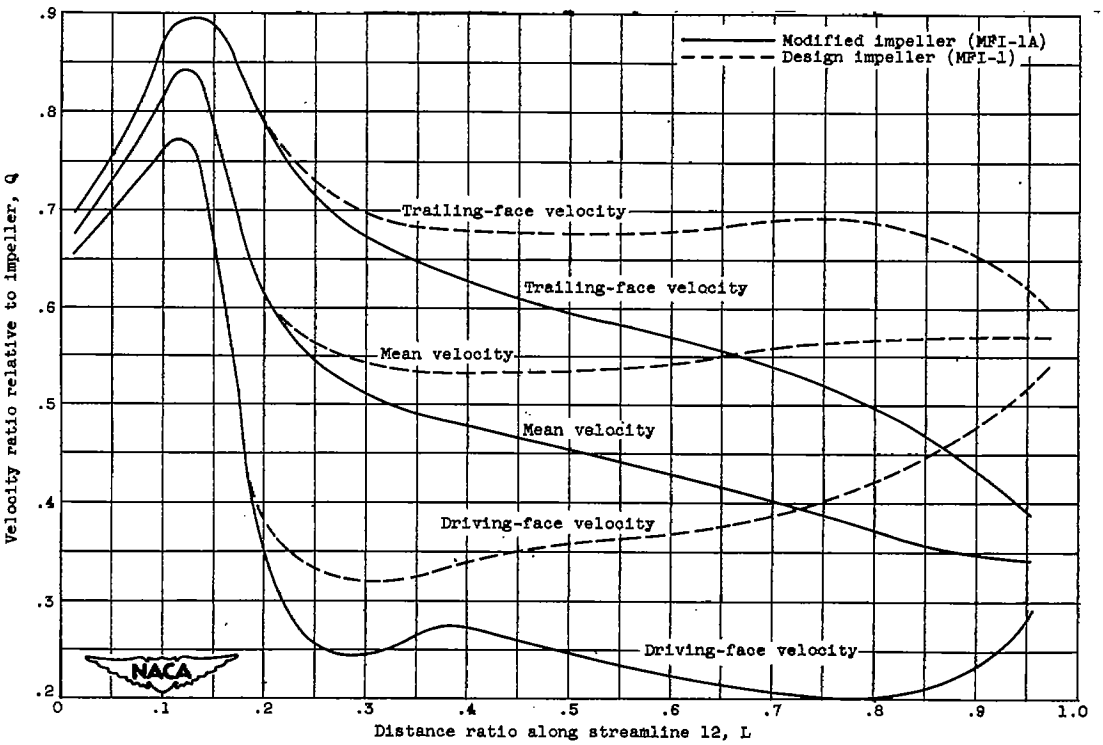

(d) Blade to blade velocity distribution along streamline 12.

Figure 14. - Continued. Flow analysis in blade to blade plane for MFI-1 and MFI-1A impellers for weight flow of 13.0 pounds per second and outlet mean-line speed of 1400 feet per second.

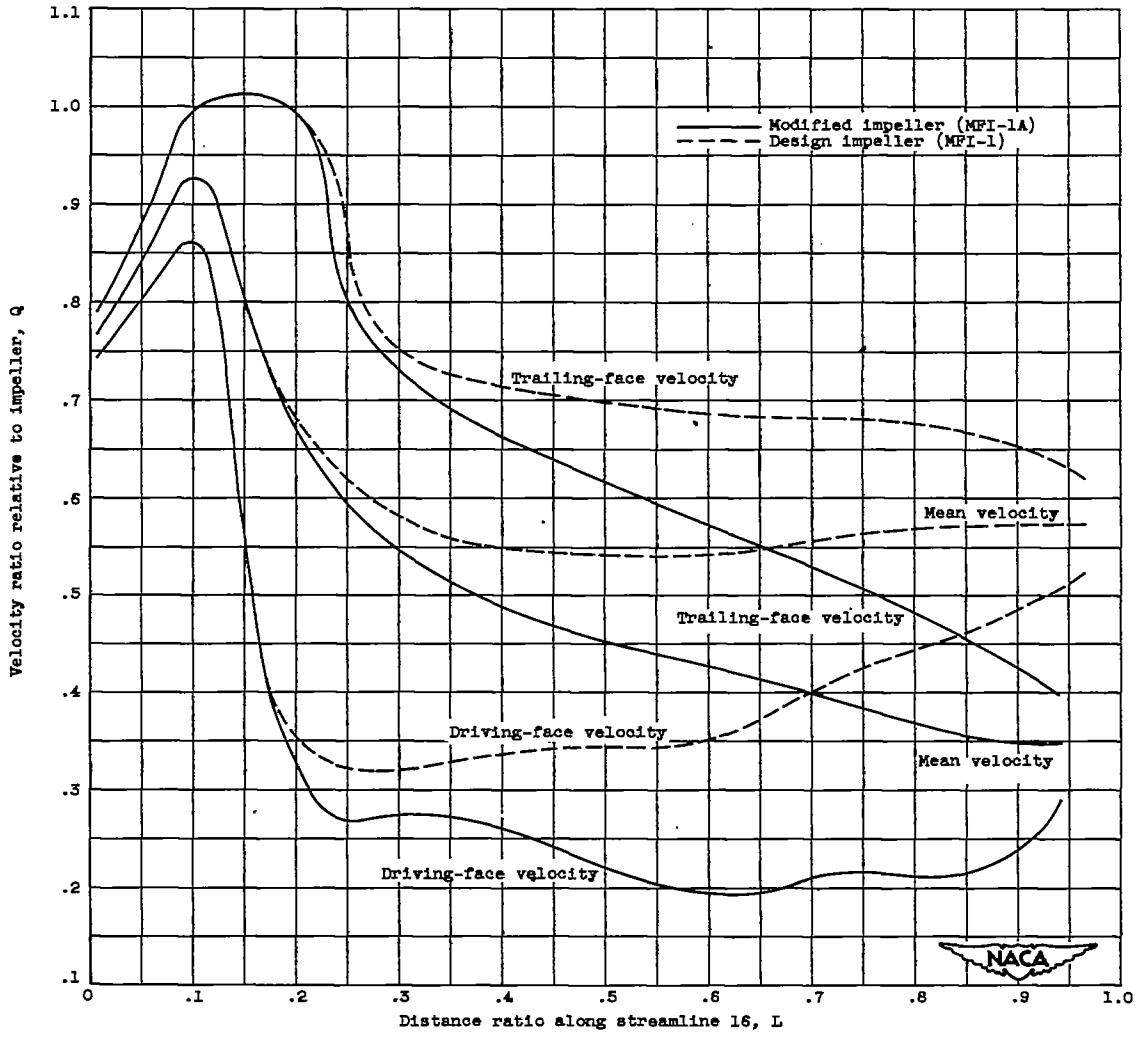

(e) Blade to blade velocity distribution along streamline 16.

Figure 14. - Continued. Flow analysis in blade to blade plane for MFI-1 and MFI-1A impellers for weight flow of 13.0 pounds per second and outlet mean-line speed of 1400 feet per second.

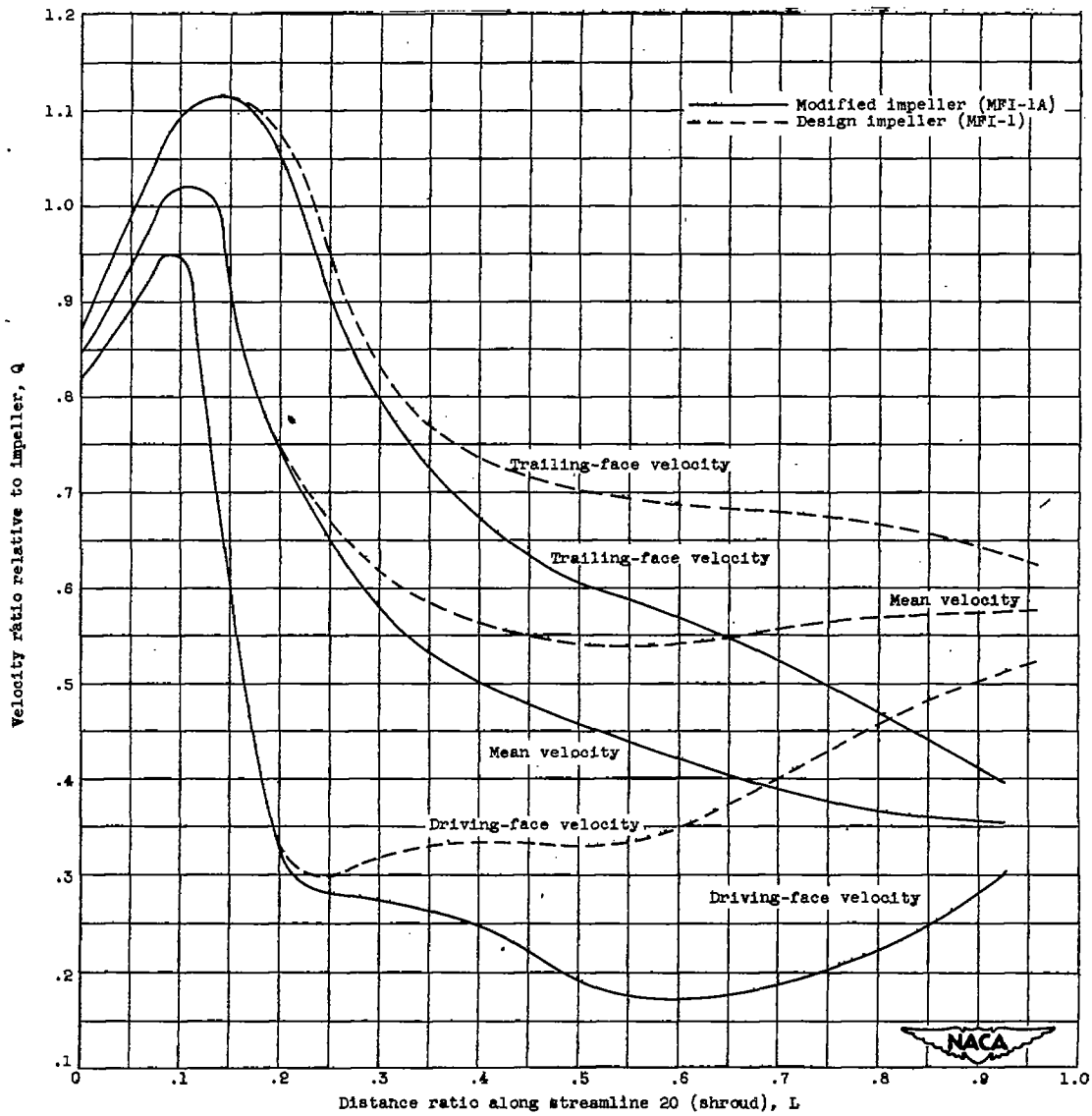

(f) Blade to blade velocity distribution along streamline 20 (shroud).

Figure 14. - Concluded. Flow analysis in blade to blade plane for MFI-1 and MFI-1A impellers for weight flow of 13.0 pounds per second and outlet mean-line speed of 1400 feet per second.

[redacted]

NACA-Langley - 9-19-52 - 400

[redacted]

[redacted]